Chapter 1:

ANGULAR MOMENTUM OPERATORS AND WAVE FUNCTIONS

1.1 DEFINITION OF ANGULAR MOMENTUM OPERATORS

Let a particle of mass m and velocity $\mathbf{v}$ be located at a position $\mathbf{r}$ measured from some origin. Then, according to classical mechanics [1], the particle has a linear momentum $\mathbf{p}$ given by

$$\mathbf{p} = m\mathbf{v} \tag{1.1}$$

and an angular momentum $\boldsymbol{\ell}$ given by

$$\boldsymbol{\ell} = \mathbf{r} \times \mathbf{p} \tag{1.2}$$

The quantum transcription [2] of Eq. (1.2) is obtained by replacing $\mathbf{p}$ by $(\hbar/i)\boldsymbol{\nabla}$, where $\hbar = h/2\pi$ is Planck's constant divided by 2π, i is the square root of minus one, and $\boldsymbol{\nabla}$ is the gradient operator whose Cartesian components are

$$\boldsymbol{\nabla} = \frac{\partial}{\partial x}\hat{\mathbf{x}} + \frac{\partial}{\partial y}\hat{\mathbf{y}} + \frac{\partial}{\partial z}\hat{\mathbf{z}} \tag{1.3}$$

In Eq. (1.3) (and elsewhere), a superscript caret denotes a unit vector. For convenience, we drop the burden of carrying around $\hbar$ by introducing a system of units in which $\hbar = 1$. Thus, the Cartesian components of $\mathbf{p}$ are

$$p_x = -i\frac{\partial}{\partial x}, \qquad p_y = -i\frac{\partial}{\partial y}, \qquad p_z = -i\frac{\partial}{\partial z} \tag{1.4}$$

and those of $\boldsymbol{\ell}$ are

$$\begin{aligned} \ell_x &= yp_z - zp_y = -i\left(y\frac{\partial}{\partial z} - z\frac{\partial}{\partial y}\right) \\ \ell_y &= zp_x - xp_z = -i\left(z\frac{\partial}{\partial x} - x\frac{\partial}{\partial z}\right) \\ \ell_z &= xp_y - yp_x = -i\left(x\frac{\partial}{\partial y} - y\frac{\partial}{\partial x}\right) \end{aligned} \tag{1.5}$$

The commutator $[\mathbf{A}, \mathbf{B}] = \mathbf{AB} - \mathbf{BA}$ of two operators $\mathbf{A}$ and $\mathbf{B}$ plays a central role in quantum mechanics [2]; the necessary condition for the observables A and B to be simultaneously measurable is that the corresponding operators $\mathbf{A}$ and $\mathbf{B}$ commute [3], that

is, $[\mathbf{A}, \mathbf{B}] = 0$. From Eq. (1.4), it is readily seen that the position vector of a particle and its momentum satisfy the basic commutation relations:

$$[x, p_x] = i, \qquad [x, p_y] = 0, \qquad [x, p_z] = 0 \tag{1.6}$$

with all cyclic permutations. Thus, for example, it is not possible to measure simultaneously along the same direction the position and linear momentum of a particle to arbitrary precision.

The commutation relations of the Cartesian components of $\boldsymbol{\ell}$ are also readily derived:

$$[\ell_x, \ell_y] = i\ell_z, \qquad [\ell_y, \ell_z] = i\ell_x, \qquad [\ell_z, \ell_x] = i\ell_y \tag{1.7}$$

Equation (1.7) has the interpretation that quantum states cannot be specified by any more than one of the labels (eigenvalues) of the three components of angular momentum. The "good" quantum numbers corresponding to the largest set of mutually commuting operators represent the maximum information that can be known about a quantum mechanical system. The measurement of another variable corresponding to an operator not commuting with this set necessarily introduces uncertainty into one of the variables already measured. A sharper specification of the system is, therefore, not possible.

Because of the importance of the commutator, it is natural to define [4] a general angular momentum operator **j** as one whose Cartesian components obey the commutation rules

$$[j_x, j_y] = ij_z, \qquad [j_y, j_z] = ij_x, \qquad [j_z, j_x] = ij_y \tag{1.8}$$

in analogy to Eq. (1.7). This extended definition returns an unexpected dividend. As we shall see in the next section, it permits the existence of spin—a quantity that has no classical analogy. We will reserve $\boldsymbol{\ell}$ for orbital angular momentum and use **j** for general angular momentum.

1.2 EIGENVALUES AND MATRIX ELEMENTS OF ANGULAR MOMENTUM OPERATORS

The square of the total angular momentum is defined as

$$\mathbf{j}^2 = j_x^2 + j_y^2 + j_z^2 \tag{1.9}$$

This operator has the commutation properties that

$$[\mathbf{j}^2, j_x] = [\mathbf{j}^2, j_y] = [\mathbf{j}^2, j_z] = 0 \tag{1.10}$$

Hence, we can construct states $|jm\rangle$ that are simultaneously eigenfunctions of $\mathbf{j}^2$ and any one component of $\mathbf{j}$, say, j_z; that is,

$$\begin{aligned} \mathbf{j}^2|jm\rangle &= \lambda_j|jm\rangle \\ j_z|jm\rangle &= m|jm\rangle \end{aligned} \tag{1.11}$$

We proceed to determine the eigenvalues $\lambda_j = \langle jm|\mathbf{j}^2|jm\rangle$ and $m = \langle jm|j_z|jm\rangle$.

The operator $j_x^2 + j_y^2 = \mathbf{j}^2 - j_z^2$ is diagonal in the $|jm\rangle$ representation. Moreover, it has positive definite (nonnegative) eigenvalues

$$\left(j_x^2 + j_y^2\right)|jm\rangle = \left(\lambda_j - m^2\right)|jm\rangle \tag{1.12}$$

because the expectation value of the square of a Hermitian operator, that is, the square of a real eigenvalue, is greater than or equal to zero. Hence, we conclude that the value of m is bounded from both above and below in that m^2 cannot exceed λ_j. This implies that for a given $\mathbf{j}$, there exist minimum and maximum values of m, denoted by $m_{\min}$ and $m_{\max}$, respectively.

Let us introduce the raising and lowering operators $j_\pm$, defined by

$$j_+ = j_x + ij_y, \qquad j_- = j_x - ij_y \tag{1.13}$$

From Eqs. (1.8) and (1.10), it is readily shown that these satisfy the commutation rules:

$$\begin{aligned} [\mathbf{j}^2, j_\pm] &= 0 \\ [j_z, j_\pm] &= \pm j_\pm \\ [j_+, j_-] &= 2\, j_z \end{aligned} \tag{1.14}$$

Let us examine the behavior of the function $j_\pm|jm\rangle$. We find

$$\mathbf{j}^2 j_\pm|jm\rangle = j_\pm \mathbf{j}^2|jm\rangle = \lambda_j j_\pm|jm\rangle \tag{1.15}$$

and

$$j_z j_\pm|jm\rangle = (j_\pm j_z \pm j_\pm)|jm\rangle = (m \pm 1) j_\pm|jm\rangle \tag{1.16}$$

Thus, $j_\pm|jm\rangle$ is an eigenfunction of $\mathbf{j}^2$ with the eigenvalue λ_j and an eigenfunction of j_z with the eigenvalue $m \pm 1$. It follows that $j_\pm|jm\rangle$ is proportional to the normalized eigenfunction $|jm \pm 1\rangle$, that is

$$j_\pm|jm\rangle = C_\pm|j\, m \pm 1\rangle \tag{1.17}$$

where $C_\pm$ is a proportionality constant. The ability of the raising and lowering operators $j_\pm$ to alter m by ± 1 unit, respectively, while preserving λ_j gives them their names. Note

that the $j_\pm$ operators are also referred to in the literature as *step-up* and *step-down operators*, *ladder operators*, or *shift operators.*

Because the values of m are bounded between $m_{\min}$ and $m_{\max}$, it follows that

$$j_+ | \, j \, m_{\max} \rangle = 0 \tag{1.18}$$

and

$$j_- | \, j \, m_{\min} \rangle = 0 \tag{1.19}$$

By applying j_- to Eq. (1.18) and j_+ to Eq. (1.19) and by using the identity

$$j_\mp j_\pm = \mathbf{j}^2 - j_z(j_z \pm 1) \tag{1.20}$$

we obtain the two equations

$$\begin{aligned} \lambda_j - m_{\max}(m_{\max} + 1) = 0 \\ \lambda_j - m_{\min}(m_{\min} - 1) = 0 \end{aligned} \tag{1.21}$$

Elimination of λ_j yields

$$m_{\max}(m_{\max} + 1) = m_{\min}(m_{\min} - 1) \tag{1.22}$$

or

$$(m_{\max} + m_{\min})(m_{\max} - m_{\min} + 1) = 0 \tag{1.23}$$

One of these two factors must vanish. Since $m_{\max} \geq m_{\min}$, the only solution to Eq. (1.23) is

$$m_{\max} = -m_{\min} \tag{1.24}$$

Successive values of m differ by unity [see Eq. (1.16)]. Therefore, $m_{\max} - m_{\min}$ is a positive definite integer, which we may denote by $2j$, where j is an integer or half-integer. Then, from $m_{\max} - m_{\min} = 2\,j$ and $m_{\max} + m_{\min} = 0$, we conclude that

$$m_{\max} = j, \qquad m_{\min} = -j \tag{1.25}$$

and there are $2j + 1$ possible values of m, $m = j,\ j - 1,\ \ldots,\ -j + 1,\ -j$ for each value of j. Substitution of Eq. (1.25) into Eq. (1.21) yields the additional result

$$\lambda_j = j(j + 1) \tag{1.26}$$

We now evaluate the proportionality constant $C_\pm$ appearing in Eq. (1.17). We find

$$\left|C_\pm\right|^2 = \langle jm | j_\mp \, j_\pm | jm \rangle = \langle jm | \mathbf{j}^2 - j_z(j_z \pm 1) | jm \rangle = j(j + 1) - m(m \pm 1) \tag{1.27}$$

where we have used Eq. (1.20) and the property that the adjoint (complex conjugate transpose) of $j_\pm$ is $j_\mp$. Note that the $j_\pm$ operators are not Hermitian, that is, not self-adjoint, although j_x, j_y, and j_z are. From Eq. (1.27), it is seen that the absolute value of $C_\pm$ is determined, but its phase is arbitrary. We choose $C_\pm$ to be real, that is,

$$C_\pm = \sqrt{j(j+1) - m(m \pm 1)} \tag{1.28}$$

This choice agrees with the standard phase convention [5], namely, that the matrix elements of j_x are real, while those of j_y are purely imaginary.

In summary, we write down all the matrix elements of the angular momentum operators in which $\mathbf{j}^2$ and j_z are diagonal:

$$\langle jm|\mathbf{j}^2|j'm'\rangle = j(j+1)\delta_{jj'}\delta_{mm'} \tag{1.29}$$

$$\langle jm|j_z|j'm'\rangle = m'\delta_{jj'}\delta_{mm'} \tag{1.30}$$

$$\langle jm|j_\pm|j'm'\rangle = \sqrt{j(j+1) - m'(m' \pm 1)}\,\delta_{jj'}\delta_{m,m'\pm 1} \tag{1.31}$$

$$\langle jm|j_x|j'm'\rangle = \tfrac{1}{2}\sqrt{j(j+1) - m'(m' \pm 1)}\,\delta_{jj'}\delta_{m,m'\pm 1} \tag{1.32}$$

$$\langle jm|j_y|j'm'\rangle = \mp\tfrac{1}{2}i\sqrt{j(j+1) - m'(m' \pm 1)}\,\delta_{jj'}\delta_{m,m'\pm 1} \tag{1.33}$$

In Eqs. (1.29)–(1.33), $\delta_{ii'}$, called the *Kronecker delta*, is defined as having the properties that $\delta_{ii'} = 0$ for $i \neq i'$ and $\delta_{ii'} = 1$ for $i = i'$.

The angular momentum quantum number j can have any of the values $0,\ \frac{1}{2},\ 1,\ \frac{3}{2},\ 2,\ \ldots$ in units of $\hbar$. Integral values of j correspond to orbital angular momenta ℓ, while half-integral values of j are referred to as *spin angular momenta*. The use of the commutation rules as the definition of the angular momentum operators puts orbital and spin angular momenta on the same footing.

1.3 ANGULAR MOMENTUM SPATIAL WAVE FUNCTIONS

So far, we have considered the angular momentum eigenfunctions $|jm\rangle$ in an abstract vector space of $2j + 1$ dimensions. For integral j, denoted by ℓ, it is often useful to work in an explicit coordinate representation for ℓ and its states $|\ell m\rangle$ by introducing the spherical polar coordinates

$$\begin{aligned} x &= r\sin\theta\cos\phi \\ y &= r\sin\theta\sin\phi \\ z &= r\cos\theta \end{aligned} \tag{1.34}$$

which have the inverse relations

$$\begin{aligned} r^2 &= x^2 + y^2 + z^2 \\ \cos\theta &= z/r \\ \tan\phi &= y/x \end{aligned} \tag{1.35}$$

Then, Eq. (1.5) becomes

$$\begin{aligned} \ell_x &= i\left(\sin\phi\ \frac{\partial}{\partial\theta} + \cot\theta\cos\phi\frac{\partial}{\partial\phi}\right) \\ \ell_y &= i\left(-\cos\phi\ \frac{\partial}{\partial\theta} + \cot\theta\sin\phi\frac{\partial}{\partial\phi}\right) \\ \ell_x &= -i\frac{\partial}{\partial\phi} \end{aligned} \tag{1.36}$$

This result is readily obtained using the nine partial derivatives, in which the appropriate *Cartesian* coordinates are held constant

$$\begin{aligned} &\frac{\partial r}{\partial x} = \sin\theta\cos\phi\,, \quad \frac{\partial r}{\partial y} = \sin\theta\sin\phi\,, \quad \frac{\partial r}{\partial z} = \cos\theta \\ &\frac{\partial\theta}{\partial x} = \frac{\cos\theta\cos\phi}{r}, \quad \frac{\partial\theta}{\partial y} = \frac{\cos\theta\sin\phi}{r}, \quad \frac{\partial\theta}{\partial z} = -\frac{\sin\theta}{r} \\ &\frac{\partial\phi}{\partial x} = -\frac{\sin\phi}{r\sin\theta}, \quad \frac{\partial\phi}{\partial y} = \frac{\cos\phi}{r\sin\theta}, \quad \frac{\partial\phi}{\partial z} = 0 \end{aligned} \tag{1.37}$$

and applying the chain rule for differentiation. For example,

$$\begin{aligned} \ell_x &= -i\left(y\frac{\partial}{\partial z} - z\frac{\partial}{\partial y}\right) \\ &= -i\left[r\sin\theta\sin\phi\ \left(\frac{\partial r}{\partial z}\frac{\partial}{\partial r} + \frac{\partial\theta}{\partial z}\frac{\partial}{\partial\theta} + \frac{\partial\phi}{\partial z}\frac{\partial}{\partial\phi}\right)\right. \\ &\quad \left. - r\cos\theta\left(\frac{\partial r}{\partial y}\frac{\partial}{\partial r} + \frac{\partial\theta}{\partial y}\frac{\partial}{\partial\theta} + \frac{\partial\phi}{\partial y}\frac{\partial}{\partial\phi}\right)\right] \\ &= -i\left[r\sin\theta\sin\phi\ \left(\cos\theta\frac{\partial}{\partial r} - \frac{\sin\theta}{r}\ \frac{\partial}{\partial\theta}\right)\right. \\ &\quad \left. - r\cos\theta\ \left(\sin\theta\sin\phi\ \frac{\partial}{\partial r} + \frac{\cos\theta\sin\phi}{r}\frac{\partial}{\partial\theta} + \frac{\cos\phi}{r\sin\theta}\frac{\partial}{\partial\phi}\right)\right] \\ &= i\ \left(\sin\phi\frac{\partial}{\partial\theta} + \cot\theta\cos\phi\frac{\partial}{\partial\phi}\right) \end{aligned} \tag{1.38}$$

as advertised, and so on. From Eq. (1.36) it follows that

$$\ell_{\pm} = e^{\pm i\phi}\left(\pm\frac{\partial}{\partial\theta} + i\cot\theta\frac{\partial}{\partial\phi}\right) \tag{1.39}$$

and

$$\boldsymbol{\ell}^2 = -\left[\frac{1}{\sin^2\theta}\frac{\partial^2}{\partial\phi^2} + \frac{1}{\sin\theta}\frac{\partial}{\partial\theta}\left(\sin\theta\frac{\partial}{\partial\theta}\right)\right] \tag{1.40}$$

In this representation, the eigenvalue problem

$$\begin{aligned}\boldsymbol{\ell}^2|\ell m\rangle &= \ell(\ell+1)|\ell m\rangle \\ \ell_z\,|\ell m\rangle &= m|\ell m\rangle\end{aligned} \tag{1.41}$$

yields two partial differential equations whose solutions are the spherical harmonic functions [2]

$$Y_{\ell m}(\theta,\phi) \equiv |\ell m\rangle \tag{1.42}$$

The spherical harmonics may be written as the product of two functions, one that depends only on the polar angle θ and the other on the azimuthal angle ϕ

$$Y_{\ell m}(\theta,\ \phi) = \Theta_{\ell m}(\theta)\Phi_m(\phi) \tag{1.43}$$

The $\Phi_m(\phi)$ functions satisfy the differential equation

$$\left[\frac{d^2}{d\phi^2} + m^2\right]\Phi_m(\phi) = 0 \tag{1.44}$$

and have the explicit form

$$\Phi_m(\phi) = \frac{1}{\sqrt{2\pi}}\exp(im\phi) \tag{1.45}$$

These functions are normalized so that

$$\int_0^{2\pi}\Phi_m^*(\phi)\Phi_{m'}(\phi)d\phi = \delta_{mm'} \tag{1.46}$$

The $\Theta_{\ell m}(\theta)$ functions satisfy the differential equation

$$\left[\frac{1}{\sin\theta}\frac{d}{d\theta}\left(\sin\theta\frac{d}{d\theta}\right) + \ell(\ell+1) - \frac{m^2}{\sin^2\theta}\right]\Theta_{\ell m}(\theta) = 0 \tag{1.47}$$

and have the explicit form for $m \geq 0$

$$\Theta_{\ell m}(\theta) = \frac{(-1)^m}{2^\ell \ell!}\sqrt{\frac{2\ell+1}{2}\frac{(\ell-m)!}{(\ell+m)!}}(\sin\theta)^m\left[\frac{d}{d(\cos\theta)}\right]^{\ell+m}(\cos^2\theta-1)^\ell \tag{1.48}$$

These functions are normalized so that

$$\int_0^\pi \Theta^*_{\ell m}(\theta)\Theta_{\ell' m}(\theta)\sin\theta\, d\theta = \delta_{\ell\ell'} \tag{1.49}$$

For many purposes, it is useful to relate the $\Theta_{\ell m}(\theta)$ to the so-called associated Legendre functions

$$P_\ell^m(\cos\theta) = \sin^m\theta\left[\frac{d}{d(\cos\theta)}\right]^m P_\ell(\cos\theta) \tag{1.50}$$

where

$$P_\ell(\cos\theta) = \frac{1}{2^\ell \ell!}\left[\frac{d}{d(\cos\theta)}\right]^\ell (\cos^2\theta - 1)^\ell \tag{1.51}$$

are the ordinary Legendre polynomials. Comparison of Eq. (1.48) with Eqs. (1.50) and (1.51) shows that we may make the identification

$$\Theta_{\ell m}(\theta) = (-1)^m\sqrt{\frac{2\ell+1}{2}\frac{(\ell-m)!}{(\ell+m)!}}P_\ell^m(\cos\theta) \tag{1.52}$$

for $m \geq 0$. For negative *m*, we choose to define

$$\Theta_{\ell,-|m|} = (-1)^m\Theta_{\ell|m|} \tag{1.53}$$

so that $\Theta_{\ell m}(\theta)$ for $m < 0$ is still given by Eq. (1.48) or (1.52) but with $|m|$ in place of *m* and the factor $(-1)^m$ omitted. This choice of phase is consistent with the previously made choice of sign concerning the matrix elements of ℓ_x and ℓ_y [5].

For the special case of *m* = 0

$$Y_{\ell 0}(\theta,\phi) = \frac{1}{\sqrt{2\pi}}\Theta_{\ell 0}(\theta) = \sqrt{\frac{2\ell+1}{4\pi}}P_\ell(\cos\theta) \tag{1.54}$$

Because $P_\ell^m(1)$ vanishes except for *m* = 0, it follows that

$$Y_{\ell m}(0,\phi) = \sqrt{\frac{2\ell+1}{4\pi}}\delta_{m0} \tag{1.55}$$

Finally, we also note that

$$Y^*_{\ell m}(\theta,\phi) = (-1)^m Y_{\ell,-m}(\theta,\phi) \tag{1.56}$$

The spherical harmonics constitute an orthonormal set over the unit sphere

$$\langle \ell m|\ell' m'\rangle = \int_0^{2\pi} d\phi \int_0^\pi \sin\theta\, d\theta\, Y^*_{\ell m}(\theta,\phi)Y_{l' m'}(\theta,\phi) = \delta_{\ell\ell'}\delta_{mm'} \tag{1.57}$$

In particular, for the special case $m = m' = 0$, we obtain the orthonormality relations for the Legendre polynomials

$$\int_0^\pi \sin\theta \, d\theta \; P_\ell(\cos\theta) P_{\ell'}(\cos\theta) = \frac{2}{2\ell+1}\delta_{\ell\ell'} \tag{1.58}$$

by substituting Eq. (1.54) into Eq. (1.57) and carrying out the integration over $d\phi$. Equation (1.57) allows us to identify $Y^*_{\ell m} Y_{\ell m} d\Omega$ with the probability that the position vector **r** points into the solid angle element $d\Omega = \sin\theta \, d\theta d\phi$ when the expectation value (average value) of ℓ_z is m. Note that $Y^*_{\ell m} Y_{\ell m}$ is independent of ϕ. This leads naturally to a geometric interpretation of ℓ as a vector making a constant projection m on the z axis when the system is in the state $|\ell m\rangle$. We discuss the implications of this statement more fully in the next section.

For reference purposes, we list the first few spherical harmonics (ℓ = 0, 1, 2, 3, 4):

$$Y_{00}(\theta,\phi) = \sqrt{\frac{1}{4\pi}}$$

$$Y_{10}(\theta,\phi) = \sqrt{\frac{3}{4\pi}}\cos\theta = \sqrt{\frac{3}{4\pi}}\frac{z}{r}$$

$$Y_{1\pm1}(\theta,\phi) = \mp\sqrt{\frac{3}{8\pi}}\sin\theta \, e^{\pm i\phi} = \mp\sqrt{\frac{3}{8\pi}}\frac{x \pm iy}{r}$$

$$Y_{20}(\theta,\phi) = \sqrt{\frac{5}{16\pi}}(3\cos^2\theta - 1) = \sqrt{\frac{5}{16\pi}}\frac{3z^2 - r^2}{r^2}$$

$$Y_{2\pm1}(\theta,\phi) = \mp\sqrt{\frac{15}{8\pi}}\sin\theta\cos\theta \, e^{\pm i\phi} = \mp\sqrt{\frac{15}{8\pi}}\frac{(x \pm iy)z}{r^2}$$

$$Y_{2\pm2}(\theta,\phi) = \sqrt{\frac{15}{32\pi}}\sin^2\theta \, e^{\pm 2i\phi} = \sqrt{\frac{15}{32\pi}}\frac{(x \pm iy)^2}{r^2}$$

$$Y_{30}(\theta,\phi) = \sqrt{\frac{7}{16\pi}}(5\cos^3\theta - 3\cos\theta) = \sqrt{\frac{7}{16\pi}}\frac{z(5z^2 - 3r^2)}{r^3}$$

$$Y_{3\pm1}(\theta,\phi) = \mp\sqrt{\frac{21}{64\pi}}\sin\theta(5\cos^2\theta - 1) \, e^{\pm i\phi} = \mp\sqrt{\frac{21}{64\pi}}\frac{(x \pm iy)(5z^2 - r^2)}{r^3}$$

$$
\begin{aligned}
Y_{3\pm2}(\theta,\phi) &= \sqrt{\frac{105}{32\pi}}\sin^2\theta\cos\theta\, e^{\pm2i\phi} = \sqrt{\frac{105}{32\pi}}\frac{(x\pm iy)^2 z}{r^3} \\
Y_{3\pm3}(\theta,\phi) &= \mp\sqrt{\frac{35}{64\pi}}\sin^3\theta\, e^{\pm3i\phi} = \mp\sqrt{\frac{35}{64\pi}}\frac{(x\pm iy)^3}{r^3} \\
Y_{40}(\theta,\phi) &= \frac{3}{16\sqrt{\pi}}(35\cos^4\theta - 30\cos^2\theta + 3) = \frac{3}{16\sqrt{\pi}}\frac{35z^4 - 30z^2r^2 + 3r^4}{r^4} \\
Y_{4\pm1}(\theta,\phi) &= \mp\frac{3}{8}\sqrt{\frac{5}{\pi}}\sin\theta(7\cos^3\theta - 3\cos\theta)\, e^{\pm i\phi} = \mp\frac{3}{8}\sqrt{\frac{5}{\pi}}\frac{(x\pm iy)(7z^3 - 3zr^2)}{r^4} \\
Y_{4\pm2}(\theta,\phi) &= \frac{3}{8}\sqrt{\frac{5}{2\pi}}\sin^2\theta(7\cos^2\theta - 1)\, e^{\pm2i\phi} = \frac{3}{8}\sqrt{\frac{5}{2\pi}}\frac{(x\pm iy)^2(7z^2 - r^2)}{r^4} \\
Y_{4\pm3}(\theta,\phi) &= \mp\frac{3}{8}\sqrt{\frac{35}{\pi}}\sin^3\theta\cos\theta\, e^{\pm i3\phi} = \mp\frac{3}{8}\sqrt{\frac{35}{\pi}}\frac{(x\pm iy)^3 z}{r^4} \\
Y_{4\pm4}(\theta,\phi) &= \frac{3}{16}\sqrt{\frac{35}{2\pi}}\sin^4\theta\, e^{\pm i4\phi} = \frac{3}{16}\sqrt{\frac{35}{2\pi}}\frac{(x\pm iy)^4}{r^4}
\end{aligned}
\tag{1.59}
$$

1.4 SPIN WAVE FUNCTIONS

It is not possible to express the basis vectors $|jm\rangle$ for half-integral values of j and m in terms of single-valued continuous functions on a unit sphere, as we just have done for $|\ell m\rangle$. However, it is possible to build up the $|jm\rangle$ from the spin eigenfunctions for $j = \frac{1}{2}$, denoted by

$$\alpha = \left|\tfrac{1}{2}\ \tfrac{1}{2}\right\rangle = \begin{pmatrix}1\\0\end{pmatrix} \tag{1.60}$$

and

$$\beta = \left|\tfrac{1}{2}\ -\tfrac{1}{2}\right\rangle = \begin{pmatrix}0\\1\end{pmatrix} \tag{1.61}$$

Using Eqs. (1.29)–(1.33), we can easily show that the angular momentum operators j_x, j_y, j_z have the 2×2 matrix representation

$$
\begin{aligned}
j_x &= \tfrac{1}{2}\sigma_x = \tfrac{1}{2}\begin{pmatrix} 0 & 1 \\ 1 & 0 \end{pmatrix} \\
j_y &= \tfrac{1}{2}\sigma_y = \tfrac{1}{2}\begin{pmatrix} 0 & -i \\ i & 0 \end{pmatrix} \\
j_z &= \tfrac{1}{2}\sigma_z = \tfrac{1}{2}\begin{pmatrix} 1 & 0 \\ 0 & -1 \end{pmatrix}
\end{aligned}
\tag{1.62}
$$

where $\sigma_x, \sigma_y, \sigma_z$ are called *Pauli spin matrices*. It follows that

$$
\begin{aligned}
j_+ &= j_x + i j_y = \begin{pmatrix} 0 & 1 \\ 0 & 0 \end{pmatrix} \\
j_- &= j_x - i j_y = \begin{pmatrix} 0 & 0 \\ 1 & 0 \end{pmatrix} \\
j^2 &= j_x^2 + j_y^2 + j_z^2 = j_z^2 - j_z + j_+ j_- = \tfrac{3}{4}\begin{pmatrix} 1 & 0 \\ 0 & 1 \end{pmatrix}
\end{aligned}
\tag{1.63}
$$

Here, α is often called *spin up* and β *spin down* for $j_z\alpha = \left(+\frac{1}{2}\right)\alpha$ and $j_z\beta = \left(-\frac{1}{2}\right)\beta$. The eigenfunctions α and β are an example of what are called *spinors* because of their special transformation properties under rotation, which are discussed in Section 3.5.

Equations (1.62) and (1.63) are one representation of the angular momentum operators. Symbolically, the operators j_+, j_-, and j_z may also be written as differential operators in this spin space

$$
j_+ = \alpha\frac{\partial}{\partial\beta}\,, \qquad j_- = \beta\frac{\partial}{\partial\alpha}, \qquad j_z = \frac{1}{2}\left(\alpha\frac{\partial}{\partial a} - \beta\frac{\partial}{\partial\beta}\right)
\tag{1.64}
$$

from which it is readily verified in terms of these spinor differential operators

$$
\begin{aligned}
j_+\alpha &= 0, \quad & j_+\beta &= \alpha \\
j_-\alpha &= \beta, \quad & j_-\beta &= 0 \\
j_z\alpha &= \tfrac{1}{2}\alpha, \quad & j_z\beta &= -\tfrac{1}{2}\beta
\end{aligned}
\tag{1.65}
$$

Combining Eqs. (1.63) and (1.64), we may express $\mathbf{j}^2$ in the notation of spinor differential operators as

$$
\mathbf{j}^2 = \tfrac{1}{4}\left(\alpha\tfrac{\partial}{\partial\alpha} + \beta\tfrac{\partial}{\partial\beta}\right)\left(\alpha\tfrac{\partial}{\partial\alpha} + \beta\tfrac{\partial}{\partial\beta} + 2\right)
\tag{1.66}
$$

from which it is easily checked that $\mathbf{j}^2\alpha = \frac{3}{4}\alpha$ and $\mathbf{j}^2\beta = \frac{3}{4}\beta$.

Using this notation, we show that an arbitrary eigenfunction $|jm\rangle$ of $\mathbf{j}^2$ and j_z may be constructed in terms of α and β by

$$|jm\rangle = \frac{(\alpha)^{j+m}(\beta)^{j-m}}{\sqrt{(j+m)!(j-m)!}} \tag{1.67}$$

This is proved at once by applying Eqs. (1.64) and (1.66) to (1.67), from which it is found that

$$\begin{aligned} j_+|jm\rangle &= \sqrt{j(j+1)-m(m+1)}|j\ m+1\rangle \\ j_-|jm\rangle &= \sqrt{j(j+1)-m(m-1)}|j\ m-1\rangle \\ j_z|jm\rangle &= m|jm\rangle \\ \mathbf{j}^2|jm\rangle &= j(j+1)|jm\rangle \end{aligned} \tag{1.68}$$

It follows that Eq. (1.67) provides a representation of the angular momentum eigenfunctions $|jm\rangle$ in terms of the spinor differential operators. Moreover, this result is valid for both integral and half-integral *j*.

1.5 THE VECTOR MODEL

The angular momentum vector **j** can never point exactly along the *z* axis. The maximum value of $\langle j_z\rangle = m$ is when *m* takes on the value *j*, while the length of the vector **j** is given by $\sqrt{\mathbf{j}\cdot\mathbf{j}} = \sqrt{\langle\mathbf{j}^2\rangle} = \sqrt{j(j+1)}$. This result is consistent with the fact that there must be an uncertainty in the values of j_x and j_y. However, as **j** becomes large, the eigenvalue of $\mathbf{j}^2$, which may be written as $j^2(1+1/j)$, approaches j^2, allowing us to make the correspondence between the quantum number *j* and the classical angular momentum for integral *j*. Indeed, the presence of the $1/j$ term is a quantum mechanical effect that reflects our inability to measure simultaneously all three components of **j** and hence specify precisely the direction of **j**.

Let us attempt to quantify this matter. The spread in the measurements of an observable *A* corresponding to the Hermitian operator **A** is conveniently described in terms of the variance of *A*, defined as

$$(\Delta A)^2 = \langle(\mathbf{A}-\langle\mathbf{A}\rangle)^2\rangle = \langle\mathbf{A}^2\rangle - \langle\mathbf{A}\rangle^2 \tag{1.69}$$

It is customary to call the positive square root of the variance of *A*, ΔA, the *uncertainty in A*. In a representation that diagonalizes **A**, $(\Delta A)^2$vanishes, and *A* can be determined with no uncertainty, that is, to arbitrary precision in principle.

Let us consider the sum of the variances of j_x and j_y in the $|jm\rangle$ representation. According to Eq. (1.69), we have $(\Delta j_x)^2 = \langle j_x^2 \rangle$ and $\left(\Delta j_y\right)^2 = \langle j_y^2 \rangle$ because $\langle j_x \rangle$ and $\langle j_y \rangle$ both vanish [see Eqs. (1.32) and (1.33)]. But $\langle \mathbf{j}^2 \rangle = \langle j_x^2 \rangle + \langle j_y^2 \rangle + \langle j_z^2 \rangle$, that is,

$$(\Delta j_x)^2 + \left(\Delta j_y\right)^2 = j(j+1) - m^2 \tag{1.70}$$

Thus, the sum of the variances $(\Delta j_x)^2 + \left(\Delta j_y\right)^2$ is constant for a given value of m. Moreover, the value of this sum reaches a minimum for $|m| = j$, that is, when the angular momentum vector points as nearly as possible along $+z$ or $-z$.

We are thus led to a picture, called the *vector model* [6], in which the eigenstate $|jm\rangle$ is represented by an angular momentum vector **j** of length $\sqrt{j(j+1)}$ that precesses about the z axis (the axis of quantization) with a constant projection m (see Figure 1.1). Thus, **j** moves in some uniform but unobservable manner on the surface of a cone whose apex half-angle θ satisfies the relation

$$\cos\theta = \frac{m}{\sqrt{j(j+1)}} \tag{1.71}$$

In this picture, the motion of **j** must be uniform so that **j** spends as much time pointing along $+x$ as along $-x$ or $+y$ as along $-y$, causing both $\langle j_x \rangle$ and $\langle j_y \rangle$ to vanish; in other words, the projection of **j** along the x and y axes averages to zero. Hence, a classical orbit is ascribed to the state $|jm\rangle$ for integral j, that is, to the state $|\ell m\rangle$. Of course, the uncertainty principle prevents us from taking this picture too literally. However, the vector model does suggest how to regard the state $|\ell m\rangle$ in the correspondence limit [6]. Because large values of the angular momentum are commonplace in molecular problems, the vector model can often give insight into the interpretation of angular momentum theory.

To explore further the implications of the vector model and the interpretation of $|\ell m\rangle$ when the orbital angular momentum ℓ becomes large, we develop an asymptotic approximation [7] to the Legendre polynomials. Eq. (1.47) may be rewritten for $m = 0$ as

$$\left[\frac{d^2}{d\theta^2} + \cot\theta\,\frac{d}{d\theta} + \ell(\ell+1)\right] P_\ell(\cos\theta) = 0 \tag{1.72}$$

The substitution

$$P_\ell(\cos\theta) = \frac{\chi_\ell(\theta)}{(\sin\theta)^{\frac{1}{2}}} \tag{1.73}$$

leads to the differential equation for χ_ℓ

$$\left[\frac{d^2}{d\theta^2} + \left(\ell + \frac{1}{2}\right)^2 + \frac{1}{4}\csc^2\theta\right] \chi_\ell(\theta) = 0 \tag{1.74}$$

which does not contain the first derivative of χ_ℓ with respect to θ and resembles a one-dimensional Schrödinger equation. For large ℓ, the term $\left(\ell+\frac{1}{2}\right)^2$ is much larger than $\frac{1}{4}\csc^2\theta$ everywhere except for angles very close to $\theta = 0$ or $\theta = \pi$. This suggests that we approximate Eq. (1.74) by the differential equation

$$\left[\frac{d^2}{d\theta^2}+\left(\ell+\frac{1}{2}\right)^2\right]\chi_\ell(\theta)=0 \tag{1.75}$$

whose solution is

$$\chi_\ell(\theta)=A_\ell\sin\left[\left(\ell+\frac{1}{2}\right)\theta+\alpha\right] \tag{1.76}$$

where A_ℓ and α are constants [8]. Thus, for large ℓ and for $\theta \gg \ell^{-1}$ and $(\pi-\theta) \gg \ell^{-1}$, we obtain

$$P_\ell(\cos\theta) \;\rightarrow\; A_\ell\frac{\sin\left[\left(\ell+\frac{1}{2}\right)\theta+\alpha\right]}{(\sin\theta)^{\frac{1}{2}}} \tag{1.77}$$

and we may also write under the same conditions [9]

$$Y_{\ell 0}(\theta,\,\phi) \;\rightarrow\; \sqrt{\frac{\ell+\frac{1}{2}}{2\pi}}A_\ell\frac{\sin\left[\left(\ell+\frac{1}{2}\right)\theta+\alpha\right]}{(\sin\theta)^{\frac{1}{2}}} \tag{1.78}$$

Thus,

$$|Y_{\ell 0}(\theta,\,\phi)|^2 \;\rightarrow\; \frac{\left(\ell+\frac{1}{2}\right)}{2\pi}A_\ell^2\frac{\sin^2\left[\left(\ell+\frac{1}{2}\right)\theta+\alpha\right]}{\sin\theta} \tag{1.79}$$

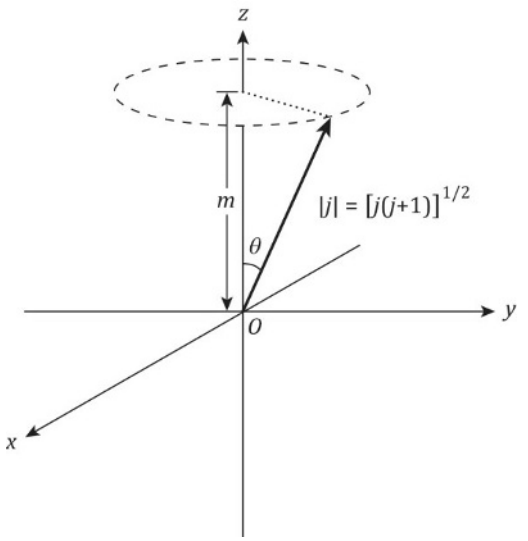

*FIGURE 1.1 Vector model for the state $|jm\rangle$, which is represented by a vector **j** that undergoes precession about the axis of quantization (the z axis), making a constant projection m on it.*

For large ℓ, the factor $\sin^2\left[\left(\ell+\frac{1}{2}\right)\theta+\alpha\right]$ oscillates very rapidly and can be replaced by its average value of $\frac{1}{2}$. Then, if we insist that the integral of $|Y_{\ell 0}(\theta,\phi)|^2$ over $d\boldsymbol{\Omega}$ be unity, we find that

$$|Y_{\ell 0}(\theta,\phi)|^2=\frac{1}{2\pi^2\sin\theta} \tag{1.80}$$

This result holds for large ℓ and for all θ except very close to $\theta=0$ and $\theta=\pi$.

We may arrive at the same result by use of the vector model. For large ℓ, the particle performs a circular orbit about $\boldsymbol{\ell}$ (see Figure 1.1); for m = 0, $\boldsymbol{\ell}$ is perpendicular to the z axis. A typical orbit is shown in Figure 1.2a. Here, θ is the angle measured about $\boldsymbol{\ell}$; ϕ is the angle measured about z (in the xy plane). The probability of finding the particle between θ and $\theta+d\theta$ is uniform. But $\boldsymbol{\ell}$, itself, may have any azimuthal orientation about z, because once we specify the values of $\boldsymbol{\ell}^2$ and ℓ_z, we cannot locate the position of $\boldsymbol{\ell}$ in the xy plane. Hence, the chance of finding $\boldsymbol{\ell}$ between ϕ and $\phi+d\phi$ is also uniform, and we must take this into account. The probability of finding the particle between θ and $\theta+d\theta$ is simply $d\theta/\pi$ because we choose θ to range from 0 to π. As ϕ is not specified, the region between θ and $\theta+d\theta$ defines a band on the unit sphere, as shown in Figure 1.2c. Then, the probability $d\theta/\pi$ must be spread over this band, which is bounded by two spherical segments, one of height $h=\cos\theta$ and the other of height $h=\cos(\theta+d\theta)$ on the unit sphere. Recall that the area of a spherical segment of radius r and height h is $2\pi rh$. The area of the band is the difference between the areas of the two spherical segments, that is, $2\pi[\cos\theta-\cos(\theta+d\theta)]=2\pi\sin\theta\,d\theta$. Thus, the probability density function is given by the probability $d\theta/\pi$ per unit area $(2\pi\sin\theta\,d\theta)$, that is, by $(2\pi^2\sin\theta)^{-1}$, in agreement with Eq. (1.80). Another way to visualize this result is to consider the density of intersections of the longitudes and latitudes on a globe (sphere). These intersections crowd together at the poles and spread apart at the equator; that is, the density of intersections is inversely proportional to $\sin\theta$.

Consider the situation for $m\neq 0$, as shown in Figure 1.2b. Here, α is the angle between $\boldsymbol{\ell}$ and the z axis, θ is the angle between the z axis, and the particle's position vector is $\mathbf{r}$, ϕ is the azimuthal angle about the z axis, and γ is the angle measured about $\boldsymbol{\ell}$. Once again, the probability of finding the particle is uniform in the angle γ, while $\boldsymbol{\ell}$ may have any azimuthal orientation about z as long as α is constant. The probability that the particle is between γ and $\gamma+d\gamma$ is $d\gamma/\pi$ because again γ is chosen to range from 0 to π; moreover, this probability is spread over the zone $2\pi\sin\theta\,d\theta$ (see Figure 1.2c). Hence, the probability density of finding the particle at some point with angle θ is $(d\gamma/\pi)/2\pi\sin\theta\,d\theta$, that is,

$$|Y_{\ell m}(\theta,\ \varphi)|^2=\left(\frac{d\gamma}{d\theta}\right)\frac{1}{2\pi^2\sin\theta} \tag{1.81}$$

In the $m = 0$ case, $\gamma = \theta$ and Eq. (1.81) reduces to Eq. (1.80), as expected.

Actually, γ is the dihedral angle [10] between the planes containing z and $\boldsymbol{\ell}$ and containing $\boldsymbol{\ell}$ and $\mathbf{r}$. We can relate γ to the angles θ and α by

$$\cos\theta = \cos\alpha \ \cos\frac{\pi}{2} + \sin\alpha \ \sin\frac{\pi}{2}\cos\gamma = \sin\alpha\cos\gamma \tag{1.82}$$

Thus,

$$\sin\theta \, d\theta = \sin\alpha \sin\gamma \ d\gamma \tag{1.83}$$

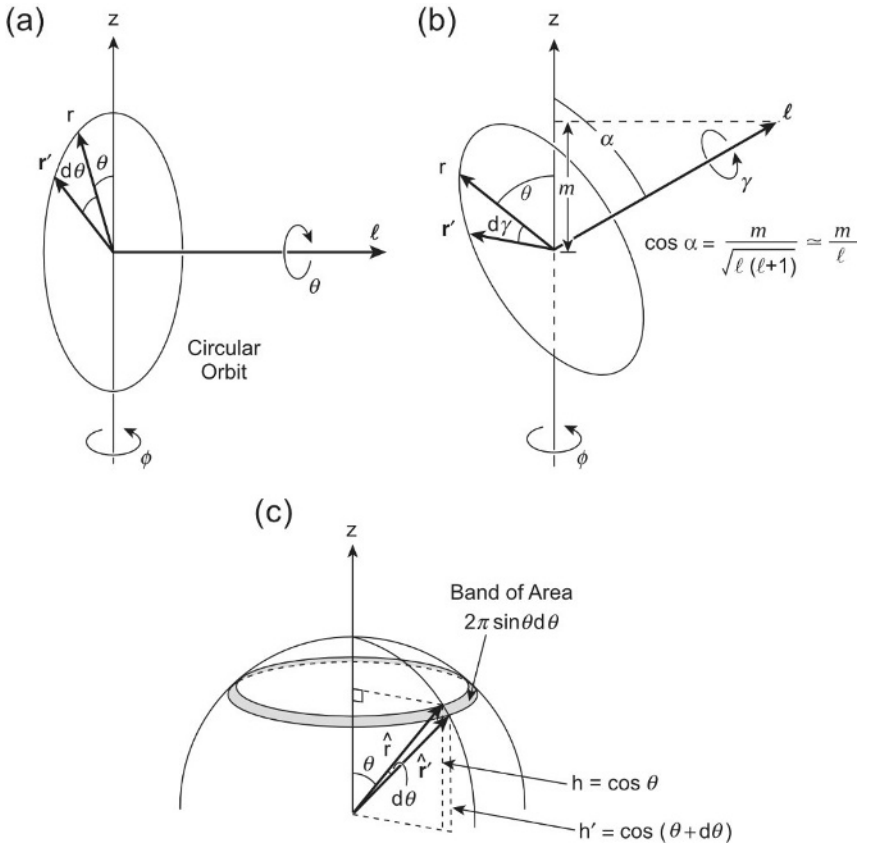

FIGURE 1.2 Classical orbits corresponding to (a) $|Y_{\ell 0}(\theta, \varphi)|^2$ and (b) $|Y_{\ell m}(\theta, \varphi)|^2$ for large ℓ. Note that $\boldsymbol{\ell}$ and $\mathbf{r}$ are perpendicular to one another. The region between θ and $\theta + d\theta$ defines a band shown in (c).

from which it follows that

$$|Y_{\ell m}(\theta,\phi)|^2 = \frac{1}{2\pi^2 \sin\alpha \sin\gamma} = \frac{1}{2\pi^2 \sin\alpha \sqrt{1-\dfrac{\cos^2\theta}{\sin^2\alpha}}}$$

$$= \frac{1}{2\pi^2\sqrt{\sin^2\alpha - \cos^2\theta}} \tag{1.84}$$

This expression holds for $\sin^2\alpha > \cos^2\theta$. The region where $\sin^2\alpha < \cos^2\theta$ corresponds to either $\theta < \frac{\pi}{2} - \alpha$ or $\theta > \frac{\pi}{2} + \alpha$ and is classically forbidden. In Figure 1.3 we present a

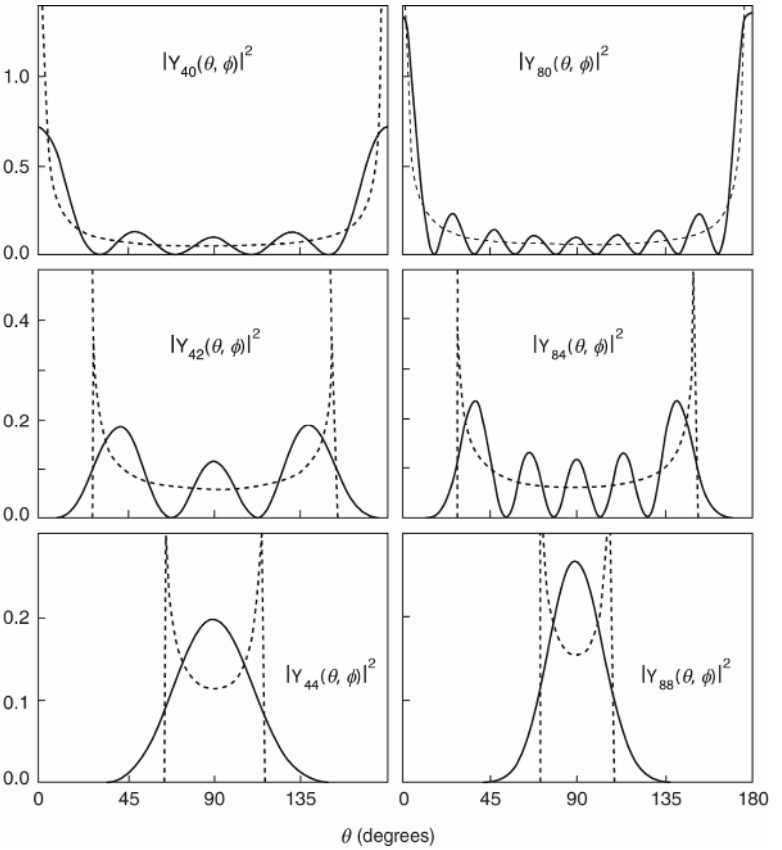

FIGURE 1.3 Probability density of $|Y_{\ell m}(\theta,\ \phi)|^2$ *as a function of θ for selected values of l and m. In each plot, the dashed curve is the semiclassical probability density given by* $1/\left[2\pi^2(sin^2\,\alpha - cos^2\,\theta)^{\frac{1}{2}}\right]$, *where* $cos^2\,\alpha = \frac{m^2}{[\ell(\ell+1)]}$. *Each curve is normalized so that* $\int_0^{2\pi}\int_0^{\pi}|Y_{\ell m}(\theta,\phi)|^2\,sin\,\theta\,d\theta\ \ d\phi = 1$.

pictorial summary of this behavior. As compared with the semiclassical limit, the quantal result for large ℓ has rapid oscillations in the classically allowed region and dies exponentially in the classically forbidden region [6]. Moreover, the quantal result rounds off the sharp singularities predicted by this semiclassical treatment. Figure 1.3 suggests the value and deficiencies of the vector model. Apart from rapid oscillations, the probability density $|Y_{\ell m}(\theta, \phi)|^2$ behaves like that of a classical particle uniformly moving in a circular orbit for large ℓ. Moreover, as shown in Figure 1.3, the vector model limit is rapidly approached as ℓ increases in magnitude.

1.6 THE RUNGE–LENZ VECTOR AND ATOMIC STRUCTURE

We conclude this chapter by taking a deeper look into the energy levels of atoms having only one electron (so-called hydrogenic atoms) and how angular momentum considerations strongly hint at the chemical periodicity of many-electron atoms (the elements). Consider an electron moving in the central force field of a proton. The classical motion is confined to a plane, and the angular momentum is perpendicular to this plane. Thus, we are free to choose the motion to be in the *xy* plane and the angular momentum to point along the *z* axis. The electron–proton system has the energy and angular momentum

$$E = \frac{p^2}{2\mu} - \frac{e^2}{r} = \frac{1}{2}\mu\left[\frac{dr}{dt}\right]^2 + \frac{L^2}{2\mu r^2} - \frac{e^2}{r} \tag{1.85}$$

$$L = \mu r^2 \frac{d\phi}{dt} \tag{1.86}$$

Taking the ratio of $d\phi/dt$ to dr/dt and integrating, we find

$$\phi = \phi_o + \int_{r_o}^{r} \frac{L/(\mu r^2)dr}{[(2/\mu)(E - L^2/(2\mu r^2) + e^2/r]^{\frac{1}{2}}} \tag{1.87}$$

where r_o and ϕ_o specify some point on the orbit of the electron about the center of mass of the electron–proton system and μ is the reduced mass. In the above, the charge on the electron is $-e$ and that on the proton is $+e$. With the substitution $x = 1/r$, we rewrite Eq. (1.87) in the form

$$\phi = \phi' + \int \frac{dx}{[2\mu E/L^2 + (2\mu e^2/L^2)x - x^2]^{\frac{1}{2}}} \tag{1.88}$$

where the integral has been put into an indefinite form by introducing the integration constant ϕ'. This indefinite integral has a standard form

$$\int \frac{dx}{\sqrt{a+bx+cx^2}} = \frac{1}{\sqrt{-c}} \arccos\left(-\frac{b+2cx}{\sqrt{b^2-4ac}}\right) \tag{1.89}$$

We can use this result to show that the orbit equation for the electron is

$$\frac{1}{r} = \frac{\mu e^2}{L^2}\left\{1 + [1 + 2EL^2/(\mu e^4)]^{1/2} \cos(\phi - \phi')\right\}$$

$$= \frac{\mu e^2}{L^2}[1 + \varepsilon \cos(\phi - \phi')] \tag{1.90}$$

This has the form of a conic section with one focus at the origin, where $\varepsilon = \sqrt{1 + 2EL^2/(\mu e^4)}$ is called the *eccentricity*. It is convenient to substitute u for $L^2/\mu e^2$. Then, the orbit equation takes the form

$$r = \frac{u}{1+\varepsilon \cos(\phi-\phi')} \tag{1.91}$$

The value of r attains a minimum value when $\phi = \phi'$. This point is called the *perihelion* of the orbit.

It is readily shown that Eq. (1.91) describes an ellipse, a parabola, or a hyperbola depending on the value of the eccentricity parameter ε. *Hint:* This task might be most easily accomplished by rotating the coordinate system to that where $\phi' = 0$ and then rewriting Eq. (1.90) in polar coordinates, $x = r\cos\phi$ and $y = r\sin\phi$ so that Eq.(1.91) becomes $(1-\varepsilon^2)\,x^2 + 2\,\varepsilon\,u\,x + y^2 = u^2$. In this rotated coordinate frame, it immediately follows that the perihelion occurs when $\phi = 0$, which locates the x axis as the line connecting the center of mass to the point of the orbit's perihelion.

For $\varepsilon > 1$, corresponding to $E > 0$, that is, scattering, we have a hyperbola; for $\varepsilon = 1$, corresponding to $E = 0$ (electron starts at rest infinitely far from the proton), the orbit is a parabola; and for $\varepsilon < 1$, corresponding to $E < 0$, that is, a bound state of the electron, the orbit is a closed ellipse. In the special case that $\varepsilon = 0$, corresponding to $E = -\mu e^4/(2L^2)$, the ellipse becomes a circular orbit.

Whenever two particles interact by means of a central force field, we have conservation of energy, linear momentum, and angular momentum. However, when the central force field has a dependence on r as the inverse square, such as for an electron and proton in a Coulomb potential, then there is an extra conserved quantity, which is often referred to as

a hidden symmetry. To appreciate this, we introduce what is called the Runge–Lenz vector [11]:

$$\mathbf{R} = \frac{1}{\mu}(\mathbf{p} \times \mathbf{L}) - e^2 \frac{\mathbf{r}}{r} \tag{1.92}$$

It can be shown that R is a constant of the motion by proving that $dR/dt = 0$.
To accomplish this task, we replace $\mathbf{L}$ by $\mathbf{r} \times \mathbf{p}$ and use the vector identity [12] $(\mathbf{A} \times \mathbf{B} \times \mathbf{C}) = (\mathbf{A} \cdot \mathbf{C})\mathbf{B} - (\mathbf{B} \cdot \mathbf{C})\mathbf{A}$. The evaluation of the time derivative of the unit vector $\hat{\mathbf{r}} = \mathbf{r}/r$ is conveniently carried out in Cartesian coordinates

$$\frac{d\hat{\mathbf{r}}}{dt} = \frac{d(\mathbf{r}/r)}{dt} = \frac{1}{r}\frac{\mathbf{p}}{\mu} + \mathbf{r}\frac{\partial(x^2 + y^2 + z^2)^{-1/2}}{\partial t} = \frac{1}{r}\frac{\mathbf{p}}{\mu} - \frac{1}{r^3}\frac{p}{\mu}\mathbf{r}$$

The Runge–Lenz vector points along the semimajor axis of the ellipse, that is, along the x axis. This conclusion is most simply seen by considering its value at the orbit's perihelion. Stated another way, the conservation of the Runge–Lenz vector is equivalent to the conservation of the position of the perihelion. In a central force field having strict r^{-2} dependence, the perihelion is fixed. If the central force field deviates slightly from r^{-2} dependence, the elliptical orbit precesses. Historically, the first evidence that the gravitational potential did not have a strict $1/r$ dependence came from astronomical observations of the precession of the perihelion of the planet mercury about the sun. Even accounting for the gravitational pull from other planets, an unexplained amount of precession remained until Einstein introduced the theory of general relativity.

We wish to establish a relationship between the three conserved quantities, E, L, and R. This task is most readily accomplished by taking the dot product of the Runge–Lenz vector with itself:

$$\begin{aligned}
\mathbf{R} \cdot \mathbf{R} = \mathbf{R}^2 &= [(\mathbf{p} \times \mathbf{L} - \mu e^2 \hat{\mathbf{r}}) \cdot (\mathbf{p} \times \mathbf{L} - \mu e^2 \hat{\mathbf{r}})]/\mu^2 \\
&= [(\mathbf{p} \times \mathbf{L}) \cdot (\mathbf{p} \times \mathbf{L}) + \mu^2 e^4 - 2\mu e^2 \mathbf{r} \cdot (\mathbf{p} \times \mathbf{L})/r]/\mu^2 \\
&= [p^2 L^2 + \mu^2 e^4 - 2\mu e^2 L^2/r]/\mu^2 \\
&= \left[2\mu L^2 \left(\frac{p^2}{2\mu} - \frac{e^2}{r}\right) + \mu^2 e^4\right]/\mu^2 \\
&= 2L^2 E/\mu + e^4
\end{aligned} \tag{1.93}$$

Here, we have used the vector identities $(\mathbf{A} \times \mathbf{B}) \cdot (\mathbf{C} \times \mathbf{D}) = (\mathbf{A} \cdot \mathbf{C})(\mathbf{B} \cdot \mathbf{D}) - (\mathbf{A} \cdot \mathbf{D})(\mathbf{B} \cdot \mathbf{C})$ and $\mathbf{A} \cdot (\mathbf{B} \times \mathbf{C}) = (\mathbf{A} \times \mathbf{B}) \cdot \mathbf{C}$. Thus, the classical hydrogen atom having an energy E is associated with an infinite number of different L and R values that satisfy the above equation. In other words, the energy of the hydrogen atom is independent of the

value of L. This same result carries over into the quantum formulation of the hydrogen atom in which the angular momentum becomes quantized, but the energy levels do not depend on the values of the angular momentum quantum number (in a nonrelativistic treatment).

In a quantum formulation of the Runge–Lenz vector, we must replace $\mathbf{p} \times \mathbf{L}$ by $(\mathbf{p} \times \mathbf{L} - \mathbf{L} \times \mathbf{p})/2$ to have a Hermitian operator:

$$\mathbf{R} = \frac{1}{2\mu}(\mathbf{p} \times \mathbf{L} - \mathbf{L} \times \mathbf{p}) - e^2\hat{\mathbf{r}} \tag{1.94}$$

Once again, it may be shown that the Hamiltonian operator, $\mathcal{H}$, commutes with the Runge–Lenz vector **R**, that is, **R** is a constant of the motion [11]. This result should be no surprise as the operators **p**, **L**, and $\hat{\mathbf{r}}$ each commute with $\mathcal{H}$.

The Hamiltonian for the H atom is

$$\mathcal{H} = \frac{p^2}{2\mu} - \frac{e^2}{r} \tag{1.95}$$

It may be shown that the following relations hold:

$$\begin{aligned}
[\mathcal{H}, L_i] &= 0 \\
[\mathcal{H}, R_i] &= 0 \\
[L_i, L_j] &= i\hbar\varepsilon_{ijk}L_k \\
[L_i, R_j] &= i\hbar\varepsilon_{ijk}R_k \\
[R_i, R_j] &= -i\hbar\varepsilon_{ijk}L_k\left[\frac{2\mathcal{H}}{\mu}\right] \\
\mathbf{R} \cdot \mathbf{L} &= \mathbf{L} \cdot \mathbf{R} = 0 \\
\mathbf{R} \cdot \mathbf{R} &= \left[\frac{2\mathcal{H}}{\mu}\right](L^2 + \hbar^2) + e^4
\end{aligned} \tag{1.96}$$

The first two commutators show that the vectors **L** and **R** are constants of the motion. The next three commutators show that **R** has the same structure as **L**, that is, acts as an angular momentum vector. The vanishing of the dot product of **R** and **L** is as expected from the classical analogs in which **R** points along the x axis and **L** along the z axis. The final relationship for the dot product of **R** with itself is more involved to work out, but is the quantum mechanical analog of Eq. (1.93) in which E has been replaced with $\mathcal{H}$ and L^2 with $L^2 + \hbar^2$. In the above, ε_{ijk}, called the Levi-Civita symbol, has the properties that it is +1 if (i, j, k) is an even (cyclic) permutation of (x, y, z), −1 if it is an odd (noncyclic) permutation, and 0 if any index is repeated. The proof of these relationships can become tedious but may be simplified by working in spherical coordinates for the Cartesian components of **r**, **p**, and **L**

For bound states of the hydrogen atom in which $E < 0$, let us rescale **R** by

$$\mathbf{A} = \sqrt{\frac{-\mu}{2E}}\mathbf{R} \tag{1.97}$$

This scaling choice causes the commutator $[A_i, A_j]$ to have the same value as the commutator $[L_i, L_j]$. The operators **A** and **L** do not commute, but the hybrid operators

$$K_{\pm} = (\mathbf{L} \pm \mathbf{A})/2 \tag{1.98}$$

do commute with each other and with the Hamiltonian. In addition,

$$\mathbf{K_+}^2 = \mathbf{K_-}^2 = \mathbf{K}^2 = (\mathbf{L}^2 + \mathbf{A}^2)/4 \tag{1.99}$$

so these two operators have the same eigenvalues. We can find the eigenvalues of the hydrogen atom without solving the Schrödinger equation, as was first accomplished by Pauli [13].

Suppose that the wave function Ψ is a simultaneous eigenfunction of $\mathbf{K}^2, K_{+z}, K_{-z}$, and $\mathcal{H}$. Then, based on the structure of a general angular momentum operator we already derived in this chapter, there is an eigenvalue $k = 0, ½, 1, ...$ such that $\mathbf{K}^2\Psi = k(k+1)\hbar^2\Psi$.

We can show that

$$\mathbf{K}^2\Psi = -\left[\frac{1}{4}\right]\left[\hbar^2 + \frac{e^4\mu}{2E}\right]\Psi \tag{1.100}$$

and therefore that

$$E = -\frac{\mu e^4}{2\hbar^2(2k+1)^2} = -\frac{\mu e^4}{2\hbar^2 n^2} \tag{1.101}$$

where $n = (2k+1)$ is called the principal quantum number.

For a given value k, there are $2k+1$ different values of both the expectations values of the K_{+z} operator and the K_{-z} operator. Hence, there are $(2k+1)^2 = n^2$ different states with the same energy for a given value of n. This degeneracy is thus a direct consequence of the hidden symmetry of the Runge–Lenz vector for the hydrogen atom. Several other cases are known of quantum systems have a conserved dynamical constant of the motion [14]. Two famous examples are the hydrogen atom in a uniform electric field and the electron motion in the H_2^+ molecule, both of which are conveniently expressed in prolate spheroidal coordinates [15].

In the hydrogen atom with principal quantum number n, there are many possible ℓ values, each of which has $2\ell + 1$ different m values associated with it. Given that the total degeneracy of a level with principal quantum number n is n^2, it follows that the ℓ values range from $\ell = 0$ to $\ell = n - 1$ in integral steps.

In the foregoing, an electron revolves around the nucleus in a specific, quantized orbit, or energy level characterized by its ℓ and n quantum numbers. Each orbit corresponds to a distinct energy level, and an electron can only exist in these discrete orbits, not in between. As we have seen, ℓ is bounded by the limits $0 \leq \ell \leq n - 1$. An electron can have spin up or spin down, so for $n = 1$, there are 2 electrons, for $n = 2$ there are 8 electrons, for $n = 3$ there are 18 electrons, and we have the beginning of understanding how the periodic table of the elements is built up. So far, we have only used angular moment considerations to build up our periodic table of the elements, and we are missing how the energy levels depend on the radial motion of the electrons. We have also only considered the behavior of one electron.

The chemical properties of an element are primarily determined by its outermost electrons, called the valence electrons. As you move through the elements, each subsequent element has one more proton in its nucleus and one more electron. The added electron goes into the lowest available energy level or shell, filling up each shell in a systematic way. When a shell is filled, the next electron must go into a new, higher energy shell, altering the element's properties significantly. For example, elements with a full outer shell (noble gases like helium, neon, and argon with 2, $2 + 8 = 10$, and $2 + 8 + 8 = 18$ electrons, respectively) are chemically inert, while elements with a single electron in a new shell (such as hydrogen with 1 electron, lithium with 3 electrons, sodium with 11 electrons, and potassium with 19 electrons) are highly reactive.

Our present considerations have not included the possible dependence of the energy on the radial motions of the electrons. If we assume that the energy ordering is in the form that the energy increases in a many-electron atom as ℓ increases, we then order the subshells within a particular n shell by $\ell = 0$ electrons, called s electrons, $\ell = 1$ electrons, called p electrons, $\ell = 2$ electrons called d electrons, and so on. By doing this, we will have built up almost correctly the periodic table, which explains so clearly why the chemical behavior of the elements has a periodic nature. The pattern of shell filling leads to periodic trends in properties like atomic radius, ionization energy, and electronegativity. Thus, a very simple model based on angular momentum properties has led to a deep insight into atomic structure and chemical reactivity.

We recognize that the above one-electron treatment provides a conceptual link between atomic structure and the periodic table, but it is also important to recognize its limitations.

It only accurately describes hydrogen-like atoms (neglecting relativistic and QED effects, such as spin–orbit coupling and the Lamb shift), and it does not account for more complex multi-electron interactions, electron spin, or sublevel filling as described in a full quantum mechanical treatment. Nevertheless, the authors are impressed by how far such a limited simple model can take us. At the end of Chapter 7, we present a similar treatment for elementary particles, recognizing full well its limitations.

NOTES [16] AND REFERENCES

1. Two of our favorite introductory texts about classical mechanics are H. Goldstein, *Classical Mechanics* (Addison-Wesley, Reading, Massachusetts, 1950) and L. D. Landau and E. M. Lifschitz, *Mechanics* (Pergamon Press, Oxford, 1960).

2. See, for example, L. Pauling and E. B. Wilson, Jr., *Introduction to Quantum Mechanics* (McGraw-Hill, New York, 1935); D. Bohm, *Quantum Theory* (Prentice Hall, Englewood Cliffs, NJ, 1951); and L. D. Landau and E. M. Lifschitz, *Quantum Mechanics* (Pergamon Press, New York, 1974).

3. If **A** and **B** are two Hermitian operators that do not commute, then the observables A and B cannot be measured simultaneously. The degree to which an inevitable lack of precision is introduced is expressed by the inequality

$$(\Delta A)(\Delta B) \geq \left|\frac{[\mathbf{A}, \mathbf{B}]}{2i}\right|$$

called the Heisenberg *uncertainty principle* [2]. Once again, the commutator has a special importance.

4. Three standard texts on angular momentum theory are indispensable to the serious student of this topic: M. E. Rose, *Elementary Theory of Angular Momentum* (Wiley, New York, 1957); A. R. Edmonds, *Angular Momentum in Quantum Mechanics* (Princeton University Press, Princeton, NJ, 1957); and D. M. Brink and G. R. Satchler, *Angular Momentum* (Clarendon Press, Oxford, 1962). The above represents a blend of these references.

5. E. U. Condon and G. H. Shortley, *Theory of Atomic Spectra* (Cambridge University Press, 1935; reprinted in paperback form, 1963). E. U. Condon once told RNZ with some disappointment that he thought that this work was most often cited for setting this phase convention! In a first encounter with phase conventions, it is tempting to take the attitude "Why should I bother because after

all, the phase is arbitrary?" Another example of a phase convention is driving a motor vehicle on the right- or left-hand side of the road. So long as you and everyone else are consistent in this choice, it certainly does not matter, but inconsistency can be detrimental to your health! This is the first of many instances where care must be exercised in the choice of phase, a most vexing aspect of angular momentum theory. Finally, a warning should be made to the uninitiated that phase conventions must be checked in going from one literature reference to another, just as one checks driving habits in going from one country to another.

6. The classical correspondence of angular momentum operators and related quantities is explored in detail by P. J. Brussaard and H. A. Tolhoek, *Physica*, **23**, 955 (1957). The vector model appears to have been first introduced by A. Sommerfeld, *Ann. Physik*, **51**, 1 (1916).

7. We follow closely here L. D. Landau and E. M. Lifschitz, *Quantum Mechanics* (Pergamon Press, London, 1958), pp. 166–168. Please note that $\cos\theta$ in Eq. (1.72) and what follows is not the same $\cos\theta$ as in Eq. (1.71) and Figure 1.1 but refers instead to the polar angle between the z axis and the particle vector **r**.

8. By replacing $\cot\theta$ by $1/\theta$ for $\theta \ll 1$ and $\ell(\ell+1)$ by $\left(\ell+\frac{1}{2}\right)^2$, Eq. (1.72) becomes

$$\left[\frac{d^2}{d\theta^2}+\frac{1}{\theta}\frac{d}{d\theta}+\left(\ell+\frac{1}{2}\right)^2\right]P_\ell(\cos\theta)=0$$

This is the differential equation satisfied by the zero-order Bessel function J_0 with argument $\left(\ell+\frac{1}{2}\right)\theta$, that is,

$$P_\ell(\cos\theta)=J_0\left[\left(\ell+\frac{1}{2}\right)\theta\right]$$

for $\theta \ll 1$. It is well known that the asymptotic expansion of the zero-order Bessel function for $x \gg 1$ is

$$J_0(x) \to \sqrt{\frac{2}{\pi x}} \sin\left(x + \frac{\pi}{4}\right)$$

Hence, we have

$$P_\ell(\cos\theta) \to \left[\frac{2}{\pi\left(\ell + \frac{1}{2}\right)\theta}\right]^{1/2} \sin\left[\left(\ell + \frac{1}{2}\right)\theta + \frac{\pi}{4}\right]$$

for $\theta\left(\ell + \frac{1}{2}\right) \gg 1$. Comparison with Eq. (1.77) permits the identification

$$A_\ell = \left[\frac{2}{\pi\left(\ell + \frac{1}{2}\right)}\right]^{1/2}$$

and $\alpha = \pi/4$. Hence, for $\theta \gg \ell^{-1}$ or $\pi - \theta \gg \ell^{-1}$

$$P_\ell(\cos\theta) = \left[\frac{2}{\pi\left(\ell + \frac{1}{2}\right)}\right]^{1/2} \frac{\sin\left[\left(\ell + \frac{1}{2}\right)\theta + \frac{\pi}{4}\right]}{\sqrt{\sin\theta}}$$

9. The condition $\left(\ell + \frac{1}{2}\right)^2 \gg \frac{1}{4}\csc^2\theta$ implies that $2\left(\ell + \frac{1}{2}\right)|\sin\theta| \gg 1$, which for small θ may be restated as $\theta\ell \gg 1$ or $(\pi - \theta)\ell \gg 1$.

10. Let the three-line segments *AO*, *BO*, and *CO* intersect at the common point *O*. Denote the included angle $\angle AOB$ by ϕ_{AOB}, $\angle AOC$ by ϕ_{AOC}, and $\angle BOC$ by ϕ_{BOC}. Then, according to spherical trigonometry, the dihedral angle ψ_{ABC}, defined as the angle between the *AOB* and *BOC* planes, is related to the ϕ values by

$$\cos\psi_{ABC} = \frac{\cos\phi_{AOC} - \cos\phi_{AOB}\cos\phi_{BOC}}{\sin\phi_{AOB}\sin\phi_{BOC}}$$

11. The history of the Runge–Lenz vector is one of many rediscoveries. See Alex Alemi, "Laplace-Runge-Lenz Vector," June, 2009 available online at: http://www.cds.caltech.edu/~marsden/wiki/uploads/projects/geomech/Alemicds205final.pdf

12. A wonderful treasure trove of vector manipulations can be found in J. W. Gibbs and E. B. Wilson, “Vector Analysis” Charles Scribner’s Sons, (New York, 1901), which is available online at: http://www.archive.org/details/vectoranalysiste00gibbiala

13. W. Pauli, *Z. Phys.* **36**, 336 (1926).

14. P. G. L. Leach and G. P. Flessas, *J. Nonlinear Math. Phys.* **10**, 340 (2003).

15. S. M. Sung and D. R. Herschbach, *J. Chem. Phys.* **95**, 7437 (1991).

16. Notes are intended to offer further information, often of a peripheral nature, in a manner that does not interrupt the flow of the main text; they are not meant to be skipped. See, for example, A. Held and P. Yodzis, *Gen. Relat. and Gravit.*, **13**, 873 (1981).

PROBLEM SET 1

1. Derive Eq. (1.20).

2. Prove Eq. (1.56).

3. In the $|jm\rangle$ representation in which $\mathbf{j}^2$ and j_z are diagonal, the matrix elements of an arbitrary operator $\boldsymbol{\mathcal{O}}$ diagonal in $\mathbf{j}^2$ are given by

$$\mathcal{O}_{mm'} = \langle jm|\boldsymbol{\mathcal{O}}|jm'\rangle$$

Thus, each such operator may be represented by a $(2j+1) \times (2j+1)$ matrix, where the rows are labeled by m and the columns by m'. Such matrices are called *representations*.

A. For the $j = 2$ case, write down explicitly the 5×5 matrices for the operators

$$j_x, j_y, j_z, j_+, j_-, \mathbf{j}^2$$

B. By carrying out the indicated matrix operations, show that

$$j_x j_y - j_y j_x = i j_z$$

C. Find the specific matrix element

$$\langle j = 2, m = 0|j_x j_y j_x|j = 2, m = 1\rangle$$

4. Given that $\langle j_z\rangle = \langle jm|j_z|jm\rangle = m$ and that m ranges from $-j$ to $+j$ in unit steps, we explore here an alternative procedure for identifying $\langle \mathbf{j}^2\rangle = \langle jm|\mathbf{j}^2|jm\rangle$ with $j(j+1)$. This is accomplished by equating the expectation value of an operator $\boldsymbol{\mathcal{O}}$ with its spatial average, defined by

$$(\boldsymbol{\mathcal{O}})_{sp} = \frac{\sum_m \langle jm|\boldsymbol{\mathcal{O}}|jm\rangle}{\sum_m \langle jm|jm\rangle} \tag{1.102}$$

Because the choice of coordinates is arbitrary and space is isotropic,

$$\langle \mathbf{j}^2\rangle = \langle j_x^2\rangle + \langle j_y^2\rangle + \langle j_z^2\rangle = 3(j_z^2)_{\text{sp}} \tag{1.103}$$

Perform the spatial average and show that $\langle \mathbf{j}^2\rangle = j(j+1)$.

Sums of the form

$$S_{2k}(j) = \sum_{m=-j}^{j} m^{2k} \tag{1.104}$$

are frequently encountered where k is an integer, but j may be integral or half-integral. We discuss here the general evaluation of Eq. (1.104). Of course, we need not bother with $S_{2k+1}(j)$ because this sum vanishes when m ranges from $-j$ to $+j$ in integral steps. We begin by examining a related problem, namely, the sums

$$S_k(n) = \sum_{i=0}^{n} i^k \tag{1.105}$$

The $k = 0$ case is particularly simple, involving just counting:

$$S_0(n) = \sum_{i=0}^{n} i^0 = \sum_{i=0}^{n} 1 = n + 1 \tag{1.106}$$

However, we may recast Eq. (1.106) into a particularly provocative form as

$$S_0(n) = \textstyle\sum_{i=0}^{n}[(i+1) - i] \tag{1.107}$$

where enumeration of this series, that is, $[1-0] + [2-1] + \cdots + [(n+1) - n]$, shows that the only surviving term is $n + 1$. This suggests a general scheme for the evaluation of $S_{k+1}(n)$ in terms of known $S_k(n)$ for k less than $k + 1$ by considering the sum $\sum_{i=0}^{n}[(i+1)^{k+1} - i^{k+1}]$, which must equal $(n+1)^{k+1}$. For example, we illustrate this procedure by deriving $S_1(n)$ with our knowledge of $S_0(n)$:

$$\sum_{i=0}^{n}[(i+1)^2 - i^2] = (n+1)^2 = \sum_{i=0}^{n}[(i^2 + 2i + 1) - i^2]$$
$$= 2S_1(n) + S_0(n) \tag{1.108}$$

from which it follows that

$$S_1(n) = \frac{(n+1)^2 - S_0(n)}{2} = \frac{(n+1)^2 - (n+1)}{2} = \frac{n(n+1)}{2} \tag{1.109}$$

In a similar manner, it is shown that

$$S_2(n) = \frac{n(n+1)(2n+1)}{6} \tag{1.110}$$

$$S_3(n) = \frac{n^2(n+1)^2}{4} \tag{1.111}$$

$$S_4(n) = \frac{n(n+1)(2n+1)\left(3n^2+3n-1\right)}{30} \tag{1.112}$$

For integral *j* we rewrite Eq. (1.104) as

$$S_{2k}(j) = 2\sum_{m=0}^{j} m^{2k} - 0^{2k} \tag{1.113}$$

and we obtain with the help of Eqs. (1.106) and (1.109)–(1.112) the following:

$$S_0(j) = 2(j+1) - 1 = 2j + 1 \tag{1.114}$$

$$S_2(j) = \frac{j(j+1)(2j+1)}{3} \tag{1.115}$$

$$S_4(j) = \frac{j(j+1)(2j+1)[3j(j+1)-1]}{15} \tag{1.116}$$

For half-integral *j*, Eq. (1.104) may be expressed as

$$S_{2k}(j) = 2\sum_{i=0}^{j-\frac{1}{2}}\left[\frac{(2i+1)}{2}\right]^{2k} \tag{1.117}$$

and explicit evaluation of Eq. (1.117) with the help of Eqs. (1.106) and (1.109)–(1.112) yields the same expressions as shown in Eqs. (1.114)–(1.116); that is, Eqs. (1.114)–(1.116) are valid for both integral and half-integral *j*. An alternative proof of the validity of Eqs. (1.114)–(1.116) for half-integral *j* is to recognize that

$$\frac{S_{2k}(j)}{2^{2k}} = S_{2k}\left(\frac{j}{2}\right) + S_{2k}\left(\frac{j}{2} - \frac{1}{2}\right) \tag{1.118}$$

5. Relation between spherical harmonics and solid harmonics.

Let us take advantage of the results from the previous exercise to construct the spherical harmonics by a method introduced by Kramers [H. A. Kramers, Quantum Mechanics. North-Holland Publishing Co., Amsterdam, 1957] and elaborated on by Powell and Crasemann [J L. Powell and B. Crasemann, Quantum Mechanics, Addison-Wesley Publishing Co., Reading, Massachusetts,

3rd printing, 1965]. The Schrödinger equation for the energy states of a particle moving in a central, spherically symmetric field of force has the form

$$\nabla^2\Psi + \frac{2m}{\hbar^2}\,[E - V(r)]\,\Psi = 0 \tag{1.119}$$

It is well known that the wave function separates into a radial part $R(r)$ and an angular part $W(\theta,\phi)$, that is, $\Psi = R(r)\,W(\theta,\phi)$. Because we are interested in only the angular part, we can set E equal to $V(r)$ for constant r with no loss of generality. Then, Eq. (1.119) becomes

$$\nabla^2 W = \left(\frac{\partial^2}{\partial x^2} + \frac{\partial^2}{\partial y^2} + \frac{\partial^2}{\partial z^2}\right) W = 0 \tag{1.120}$$

Solutions of this equation are called solid harmonics. A single-valued solid harmonic function continuous near the origin can be approximated arbitrarily well by a polynomial in *x*, *y*, and *z* in which each term is of the same degree, that is, by a homogeneous polynomial of degree *l*,

$$W_l = \sum_{p+q+r=l} a_{pqr} x^p y^q z^r \tag{1.121}$$

where *l* is an integer 0, 1, 2, etc. The coefficients a_{pqr} must be chosen so that Eq. (1.120) is satisfied.

Show that the number of linearly independent polynomials of degree *l* is given by

$(l + 1)(l + 2)/2$.

$\nabla^2 W_l$ must be a polynomial of degree $l - 2$ to satisfy Eq. (1.120). It follows that for Eq. (1.120) to hold, $(l - 1)\,l\,/2$ constraints are imposed on the coefficients a_{pqr}.

Show that the resulting number of linearly independent solid harmonic polynomials of degree *l* is given by $2\,l + 1$.

Because each term in Eq. (1.121) is proportional to r^l, W_l can be written

$$W_l = r^l Y_l \tag{1.122}$$

where Y_l is a spherical harmonic of order *l*. These W_l functions vanish as r approaches zero. In general, the Y_l functions are chosen to be a real function of the Cartesian coordinates, which is readily obtained as a linear combination of the two functions $Y_{lm}(\theta,\phi)$ and $Y_{l-m}(\theta,\phi)$ introduced earlier in spherical coordinates. The Y_l are commonly denoted by

$$\boldsymbol{Y_0}: \qquad s = \sqrt{\frac{1}{4\pi}} = Y_{0,0}$$

$$\boldsymbol{Y_1}: \qquad p_x = \sqrt{\frac{3}{4\pi}}\frac{x}{r} = \sqrt{\frac{1}{2}}\left(Y_{1,-1} - Y_{1,1}\right)$$

$$p_y = \sqrt{\frac{3}{4\pi}}\frac{y}{r} = i\sqrt{\frac{1}{2}}\left(Y_{1,-1} + Y_{1,1}\right)$$

$$p_z = \sqrt{\frac{3}{4\pi}}\frac{z}{r} = Y_{1,0}$$

$$\boldsymbol{Y_2}: \quad d_{xy} = \sqrt{\frac{15}{4\pi}}\frac{xy}{r^2} = i\sqrt{\frac{1}{2}}\left(Y_{2,-2} - Y_{2,2}\right)$$

$$d_{x^2-y^2} = \frac{1}{2}\sqrt{\frac{15}{4\pi}}\frac{x^2-y^2}{r^2} = \sqrt{\frac{1}{2}}\left(Y_{2,-2} + Y_{2,2}\right)$$

$$d_{xz} = \sqrt{\frac{15}{4\pi}}\frac{xz}{r^2} = \sqrt{\frac{1}{2}}\left(Y_{2,-1} - Y_{2,1}\right)$$

$$d_{yz} = \sqrt{\frac{15}{4\pi}}\frac{yz}{r^2} = i\sqrt{\frac{1}{2}}\left(Y_{2,-1} + Y_{2,1}\right)$$

$$d_{z^2} = \frac{1}{2}\sqrt{\frac{5}{4\pi}}\frac{2z^2-x^2-y^2}{r^2} = \frac{1}{4}\sqrt{\frac{5}{\pi}}\frac{3z^2-r^2}{r^2} = Y_{2,0}$$

$$\boldsymbol{Y_3}: \quad f_{(3x^2-y^2)y} = \frac{1}{4}\sqrt{\frac{35}{2\pi}}\frac{(3x^2-y^2)y}{r^3} = i\sqrt{\frac{1}{2}}\left(Y_{3,-3} - Y_{3,3}\right)$$

$$f_{(x^2-3y^2)x} = \frac{1}{4}\sqrt{\frac{35}{2\pi}}\frac{(x^2-3y^2)x}{r^3} = \sqrt{\frac{1}{2}}\left(Y_{3,-3} + Y_{3,3}\right)$$

$$f_{xyz} = \sqrt{\frac{105}{4\pi}}\frac{xyz}{r^3} = i\sqrt{\frac{1}{2}}\left(Y_{3,-2} - Y_{3,2}\right)$$

$$f_{(x^2-y^2)z} = \frac{1}{4}\sqrt{\frac{105}{\pi}}\frac{(x^2-y^2)z}{r^3} = \sqrt{\frac{1}{2}}\left(Y_{3,-2} + Y_{3,2}\right)$$

$$f_{x(4z^2-x^2-y^2)} = \frac{1}{4}\sqrt{\frac{21}{2\pi}}\frac{x(4z^2-x^2-y^2)}{r^3} = \sqrt{\frac{1}{2}}\left(Y_{3,-1} - Y_{3,1}\right)$$

$$f_{y(4z^2-x^2-y^2)} = \frac{1}{4}\sqrt{\frac{21}{2\pi}}\frac{y(4z^2-x^2-y^2)}{r^3} = i\sqrt{\frac{1}{2}}\left(Y_{3,-1} + Y_{3,1}\right)$$

$$f_{z^3} = \frac{1}{4}\sqrt{\frac{7}{\pi}}\frac{z\,(2z^2-3x^2-3y^2)}{r^3} = \frac{1}{4}\sqrt{\frac{7}{\pi}}\frac{z\,(5z^2-3r^2)}{r^3} = Y_{3,0}$$

***Y*₄:** $g_{xy(x^2-y^2)} = \frac{3}{4}\sqrt{\frac{35}{\pi}}\frac{xy(x^2-y^2)}{r^4} = i\sqrt{\frac{1}{2}}\left(Y_{4,-4} - Y_{4,4}\right)$

$$g_{x^4+y^4} = \frac{3}{16}\sqrt{\frac{35}{\pi}}\frac{x^2(x^2-3y^2)-y^2(3x^2-y^2)}{r^4} = \sqrt{\frac{1}{2}}\left(Y_{4,-4} + Y_{4,4}\right)$$

$$g_{x^3z} = \frac{3}{4}\sqrt{\frac{35}{2\pi}}\frac{(x^2-3y^2)xz}{r^4} = \sqrt{\frac{1}{2}}\left(Y_{4,-3} - Y_{4,3}\right)$$

$$g_{y^3z} = \frac{3}{4}\sqrt{\frac{35}{2\pi}}\frac{(3x^2-y^2)\,y\,z}{r^4} = i\sqrt{\frac{1}{2}}\left(Y_{4,-3} + Y_{4,3}\right)$$

$$g_{xyz^2} = \frac{3}{4}\sqrt{\frac{5}{\pi}}\frac{xy(7z^2-r^2)}{r^4} = i\sqrt{\frac{1}{2}}\left(Y_{4,-2} - Y_{4,2}\right)$$

$$g_{(x^2-y^2)z^2} = \frac{3}{8}\sqrt{\frac{5}{\pi}}\frac{(x^2-y^2)(7z^2-r^2)}{r^4} = \sqrt{\frac{1}{2}}\left(Y_{4,-2} + Y_{4,2}\right)$$

$$g_{xz^3} = \frac{3}{4}\sqrt{\frac{5}{2\pi}}\frac{xz(7z^2-r^2)}{r^4} = \sqrt{\frac{1}{2}}\left(Y_{4,-1} - Y_{4,1}\right)$$

$$g_{yz^3} = \frac{3}{4}\sqrt{\frac{5}{2\pi}}\frac{yz(7z^2-r^2)}{r^4} = i\sqrt{\frac{1}{2}}\left(Y_{4,-1} + Y_{4,1}\right)$$

$$g_{z^4} = \frac{3}{16}\sqrt{\frac{1}{\pi}}\frac{35z^4-30z^2r^2+3r^4}{r^4} = Y_{4,0} \qquad (1.123)$$

Images of the shapes of the orbitals are readily constructed from the above, and many examples can be found on the Internet. The following are a few illustrative examples of what the *s*, *p*, and *d* functions look like:

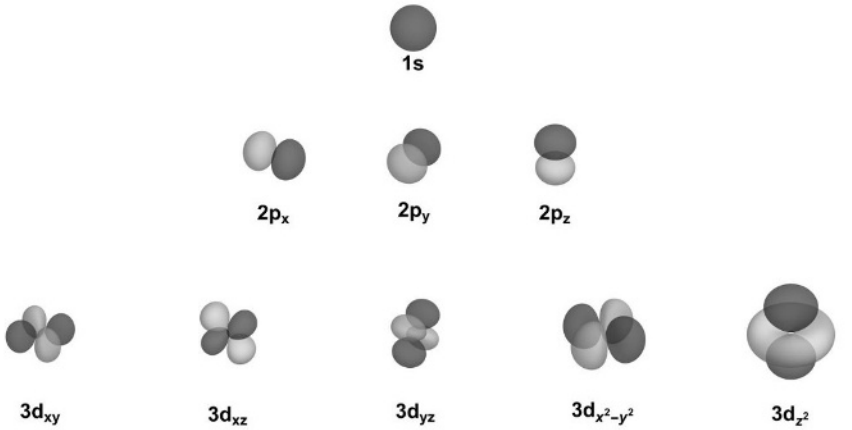

6. Derivation of the spherical harmonics made easy

Often much labor is spent developing the spherical harmonics in terms of the solutions to famous differential equations with appropriate boundary conditions. This approach can be avoided, however, by using the raising and lowering operators introduced in Eq. (1.39). For example, we already know that $L_z Y_{\ell\ell} = \ell Y_{\ell\ell}$ and $L_+ Y_{\ell\ell} = 0$.

A. Use the expression for the operators L_z and L_+ in differential form [Eqs. (1.36) and (1.39)] to show that

$$Y_{\ell\ell}(\theta,\phi) = C\left(\sin\theta\, e^{i\phi}\right)^{\ell} \tag{1.124}$$

where C is a proportionality constant.

B. Use the orthonormality condition expressed by Eq. (1.57) to show that

$$C = \frac{(-1)^{\ell}}{2^{\ell}\ell!}\sqrt{\frac{(2\ell+1)!}{4\pi}} \tag{1.125}$$

where the arbitrary phase has been chosen once again to agree with that of Condon and Shortley [5]. It follows that we have found an explicit form of the spherical harmonic of order ℓ having the largest m value:

$$Y_{\ell\ell}(\theta,\phi) = \frac{(-1)^{\ell}}{2^{\ell}\ell!}\sqrt{\frac{(2\ell+1)!}{4\pi}}(\sin\theta\, e^{i\phi})^{\ell} \tag{1.126}$$

C. The general spherical harmonic $Y_{\ell m}$ (where $m = -\ell, -\ell+1, \ldots, \ell$) is then found by $\ell - m$ successive applications of the lowering operator L_- to $Y_{\ell\ell}$:

$$Y_{\ell m}(\theta,\phi) = K(L_-)^{\ell-m} Y_{\ell\ell}(\theta,\phi) \tag{1.127}$$

where K is another proportionality constant. Using

$$L_\pm Y_{\ell m} = \sqrt{(\ell \mp m)(\ell \pm m + 1)}\, Y_{\ell m\pm 1} \tag{1.128}$$

show that

$$K = \sqrt{\frac{(\ell+m)!}{(2\ell)!(\ell-m)!}} \tag{1.129}$$

from which it follows that

$$Y_{\ell m}(\theta,\phi) = \sqrt{\frac{(\ell+m)!}{(2\ell)!(\ell-m)!}}\,(L_-)^{\ell-m} Y_{\ell\ell}(\theta,\phi) \tag{1.130}$$

D. Use Eq. (1.39) to show that the general expression for a spherical harmonic may then be written:

$$Y_{\ell m}(\theta,\phi) = (-1)^m \sqrt{\frac{(2\ell+1)(\ell+m)!(\ell-m)!}{4\pi}}\, e^{im\phi} \sum_k \frac{(-1)^k (\sin\theta)^{2k+m} (\cos\theta)^{\ell-m-2k}}{2^{2k+m}(k+m)!k!(\ell-m-2k)!} \tag{1.131}$$

This expression is readily converted into a Cartesian representation using the identity

$$e^{im\phi}(\sin\theta)^{2k+m} = \left(e^{i\phi}\sin\theta\right)^{k+m}\left(e^{-i\phi}\sin\theta\right)^{k} = (x+iy)^{k+m}(x-iy)^k \tag{1.132}$$

which yields

$$Y_{\ell m}(x,y,z) = \sqrt{\frac{(2\ell+1)(\ell+m)!\,(\ell-m)!}{4\pi}} \sum_k \frac{(-1)^{k+m}(x+iy)^{k+m}(x-iy)^k z^{\ell-m-2k}}{2^{2k+m}(k+m)!\,k!\,(\ell-m-2k)!} \tag{1.133}$$

The solid harmonics with real arguments are readily formed from the above expression by taking the appropriate linear combinations of $Y_{\ell m}$ and $Y_{\ell -m}$, as shown in Eq. (1.123).

7. Expressing the linear momentum operator in spherical polar coordinates

In a system of units with $\hbar$=1, show that

$$\begin{aligned} p_x &= -i\left[\sin\theta\cos\phi\frac{\partial}{\partial r}+\frac{\cos\theta\cos\phi}{r}\frac{\partial}{\partial\theta}-\frac{\sin\phi}{r\sin\theta}\frac{\partial}{\partial\phi}\right] \\ p_y &= -i\left[\sin\theta\sin\phi\frac{\partial}{\partial r}+\frac{\cos\theta\sin\phi}{r}\frac{\partial}{\partial\theta}+\frac{\cos\phi}{r\sin\theta}\frac{\partial}{\partial\phi}\right] \\ p_z &= -i\left[\cos\theta\frac{\partial}{\partial r}-\frac{\sin\theta}{r}\frac{\partial}{\partial\theta}\right] \end{aligned} \tag{1.134}$$

Hint: Apply the identities

$$\begin{aligned} \frac{\partial}{\partial x} &= \frac{\partial r}{\partial x}\frac{\partial}{\partial r}+\frac{\partial\theta}{\partial x}\frac{\partial}{\partial\theta}+\frac{\partial\phi}{\partial x}\frac{\partial}{\partial\phi} \\ \frac{\partial}{\partial y} &= \frac{\partial r}{\partial y}\frac{\partial}{\partial r}+\frac{\partial\theta}{\partial y}\frac{\partial}{\partial\theta}+\frac{\partial\phi}{\partial y}\frac{\partial}{\partial\phi} \\ \frac{\partial}{\partial z} &= \frac{\partial r}{\partial z}\frac{\partial}{\partial r}+\frac{\partial\theta}{\partial z}\frac{\partial}{\partial\theta}+\frac{\partial\phi}{\partial z}\frac{\partial}{\partial\phi} \end{aligned} \tag{1.135}$$

to Eq. (1.4).

APPLICATION 1:
SCATTERING THEORY

Angular momentum plays an important role in describing and understanding collision processes in addition to the dynamical behavior of bound systems. The following is intended as a cursory introduction to the beautiful topic of elastic scattering as well as a good review of many aspects of Chapter 1. First a classical treatment is presented, then a quantum one; finally, their connection is briefly outlined.

Classical Treatment

The quantum corrections to the bulk behavior of gases, such as transport or equilibrium properties, are normally rather unimportant except for light gases at low temperatures [1, 2]. In contrast, scattering experiments are a much more delicate tool for observing two-body interactions. As we shall see later, quantum mechanics does play an essential role in many scattering effects. Nevertheless, classical mechanics can illuminate the outline of this subject, is more intuitive, and thus provides a useful conceptual framework.

In the center-of-mass frame, a collision may be pictured as the interaction of a mass point μ with a central force potential $V(r)$, chosen to be located at the origin. The position vector $\mathbf{r}$ describes the location of the mass point with respect to the origin. Then, the angular momentum about the origin is given by

$$\mathbf{L} = \mathbf{r} \times \mathbf{p} = \mu(\mathbf{r} \times \dot{\mathbf{r}}) \tag{1}$$

and the time rate of change of $\mathbf{L}$ is

$$\dot{\mathbf{L}} = \mu \frac{d}{dt}(\mathbf{r} \times \dot{\mathbf{r}}) = \mu[(\dot{\mathbf{r}} \times \dot{\mathbf{r}}) + (\mathbf{r} \times \ddot{\mathbf{r}})] = 0 \tag{2}$$

for the force $\mu\ddot{\mathbf{r}}$ is always directed along $\mathbf{r}$ if the potential $V(r)$ is only a function of the magnitude of $\mathbf{r}$. Hence, $\mathbf{L}$ is a vector of constant length, that is, a conserved quantity during the collision. As $\mathbf{r}$ and $\dot{\mathbf{r}}$ must both be perpendicular to the fixed direction of $\mathbf{L}$ in space, the trajectory of the mass point is confined to a plane perpendicular to $\mathbf{L}$. This argument does not appear to hold if $\mathbf{L} = 0$, but then the motion must be along a straight line through the origin as $\mathbf{L} = \mathbf{0}$ requires $\mathbf{r}$ and $\dot{\mathbf{r}}$ to be parallel. Thus, central force motion may always be regarded as motion in a plane. We arbitrarily choose the z axis along $\mathbf{L}$ so that the trajectory is confined to the xy plane.

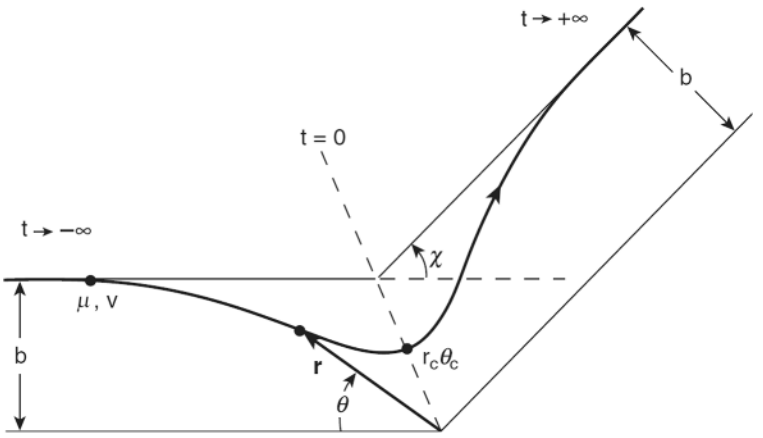

FIGURE A1.1: Elastic scattering trajectory.

A typical trajectory is pictured in Figure A1.1. For elastic scattering, the initial and final asymptotic motions differ only in the direction of the velocity **v**, which has been rotated through the angle χ, called *the deflection angle*. The asymptotic speed v and impact parameter b (which is the distance of closest approach if $V(r) = 0$) are related to the total energy E and the magnitude of the angular momentum L by

$$E = \frac{1}{2}\mu v^2 \tag{3}$$

and

$$L = \mu|\mathbf{r} \times \dot{\mathbf{r}}| = \mu v b \tag{4}$$

Note that the trajectory is symmetric about the point of closest approach ($r = r_c$, $\theta = \theta_c$). We choose $t = 0$ at this point.

Conservation of angular momentum provides three independent constants of the motion, one for each Cartesian component of **L**. Two of these suffice to express the direction of **L**, which is constant during the trajectory, and the third determines the magnitude. An additional constant of the motion, the total energy E, is provided by conservation of energy $E = T + V$, where $T = \frac{1}{2}\mu\dot{\mathbf{r}} \cdot \dot{\mathbf{r}}$ is the kinetic energy and $V = V(r)$ is the potential energy.

A. Show that

$$L = \mu r^2 \dot{\theta} \tag{5}$$

and

$$E = \frac{1}{2}\mu\left(\dot{r}^2 + r^2\dot{\theta}^2\right) + V(r) \tag{6}$$

Hint: Introduce polar coordinates

$$x = r\cos\theta$$
$$y = r\sin\theta$$

to describe the motion in the scattering plane and evaluate

$$L = \mu(x\dot{y} - y\dot{x})$$
$$E = \frac{1}{2}\mu(\dot{x}^2 + \dot{y}^2) + V(r)$$

By eliminating $\dot{\theta}$ in Eqs. (5) and (6), we obtain an equation for the radial motion

$$E = \tfrac{1}{2}\mu\dot{r}^2 + V(r) + \frac{L^2}{2\mu r^2} \tag{7}$$

Equation (7) describes the one-dimensional motion of a particle of mass μ, with total energy E in an effective potential

$$U_L(r) = V(r) + \frac{L^2}{2\mu r^2} \tag{8}$$

composed of the "true" potential $V(r)$ and the centrifugal potential $L^2/2\mu r^2$. In molecular scattering, the influence of the centrifugal potential is often dominant. The reason is that large values of L, corresponding to large impact parameters, often contribute most to the scattering process. The effective radial force is given by

$$\mu\ddot{r} = -\frac{\partial U_L}{\partial r} = -\frac{\partial V}{\partial r} + \frac{L^2}{\mu r^3} \tag{9}$$

We observe that the centrifugal contribution is always repulsive, whereas that from $V(r)$ is usually attractive for large r but repulsive for small r.

The complete solution for the scattering motion can be obtained from Eqs. (5) and (7) by integrating the differential equations

$$dr = \pm\sqrt{\frac{2}{\mu}\left(E - V(r) - \frac{L^2}{2\mu r^2}\right)}\,dt \tag{10}$$

$$d\theta = \frac{L}{\mu r^2}\,dt \tag{11}$$

and taking into account the initial starting conditions of r and θ. Hence, in the center-of-mass frame, a classical trajectory is specified by six parameters, the three Cartesian position vectors and three Cartesian velocity vectors of the representative mass point μ, or alternatively, the direction and magnitude of **L**, the value of the total

energy E and the initial values of r and θ. However, we are not interested in the complete time-dependent solution but instead in the one observable of elastic scattering, namely, the deflection angle χ. From Eqs. (10) and (11), we find

$$\theta(r) = \int_0^\theta d\theta = -\int_\infty^r \frac{(L/\mu r^2)dr}{\sqrt{(2/\mu)(E - V - L^2/2\mu r^2)}}$$
$$= -b\int_\infty^r \frac{dr}{r^2\sqrt{1 - b^2/r^2 - V/E}} \tag{12}$$

where the collision starts at $t = -\infty$, where $\theta = 0$ and $r = \infty$. Note that in Eq. (12), the square root in Eq. (10) is taken with a negative sign since $dr/d\theta$ is negative.

With respect to the angle of closest approach, θ_c,

$$2\theta_c + \chi = \pi \tag{13}$$

Hence, the angle of deflection is given by

$$\chi = \pi - 2\int_{r_c}^\infty \frac{(L/\mu r^2)dr}{\sqrt{(2/\mu)(E - V - L^2/2\mu r^2)}}$$
$$= \pi - 2b\int_{r_c}^\infty \frac{dr}{r^2\sqrt{1 - b^2/r^2 - V/E}} \tag{14}$$

where the radial distance of closest approach is determined from the condition that $dr/d\theta = 0$ or equivalently $\dot{r} = 0$. From Eq. (7) we have

$$E = \frac{L^2}{2\mu r_c^2} + V(r_c) \tag{15}$$

which may be restated as

$$b^2 = r_c^2\left[1 - \frac{V(r_c)}{E}\right] \tag{16}$$

B. Derive Eq. (16) from Eq. (15).

Once the potential function $V(r)$ is specified, the deflection angle χ may be calculated by using Eq. (14). Moreover, if $V(r_c) < 0$ (attractive potential at the turning point of the

radial motion), then $r_c < b$, whereas if $V(r_c) > 0$ (repulsive potential at the turning point), $r_c > b$.

Consider a beam of particles incident on some scattering center. Collisions occur with all possible impact parameters (angular momenta), giving rise to a corresponding distribution in angles of scattering, which is described by a *differential cross section.* Let the intensity of the incident beam be characterized in terms of the flux I_0, where I_0 is the number of particles crossing a unit area normal to the beam direction per unit time. The differential cross section $I(\chi)$ is defined so that $I(\chi)d\mathbf{\Omega}$ is the number of particles per unit time scattered into a solid angle element $d\mathbf{\Omega}$ divided by the incident flux. Note that $I(\chi)$ has the dimensions of area per steradian.

Because of the spherical symmetry of the force field, the deflection pattern is axially symmetric about the incident beam direction. Hence, $I(\chi)$ depends only on χ. Accordingly, the solid angle element $d\mathbf{\Omega}$ may be taken between the cones defined by χ and $\chi + d\chi$, that is, $d\mathbf{\Omega} = 2\pi \sin\chi \, d\chi$. Even if the force field were nonspherical, the averages over all possible impact parameters and all orientations of the target would cause any azimuthal dependence to vanish unless one of the reactants were initially polarized.

For a given initial velocity v, the fraction of the incident flux with impact parameter between b and $b + db$ is $2\pi b db$; these particles undergo deflections between χ and $\chi + d\chi$ if $d\chi/db > 0$ or between χ and $\chi - d\chi$ if $d\chi/db < 0$. This gives the relation $I(\chi)d\mathbf{\Omega} = 2\pi b db$, from which it follows that

$$I(\chi) = \frac{b}{\sin\chi \left|\frac{d\chi}{db}\right|} \tag{17}$$

where χ is related to b through Eq. (14). Hence, a knowledge of $\chi(b)$ for a given v serves to determine the differential cross section, $I(\chi)$. This is related to the *total cross section* σ by

$$\sigma = 2\pi \int_0^\pi I(\chi) \sin\chi \, d\chi \tag{18}$$

where we disregard the possibility of divergence. Hence, σ is a measure of the probability for removal by scattering from the incident beam (i.e., attenuation) and σ has the dimensions of area.

C. Consider scattering from an impenetrable sphere of radius a so that

$$V(r) = \infty, \quad r < a$$
$$V(r) = 0, \quad r > a$$

Show that the classical differential cross section is independent of the deflection angle and that the classical total cross section is just the area of a circle (bull's eye) of radius *a*. *Hint*: Begin by proving that $\chi = 2\arccos(b/a)$ for $b \leq a, \chi = 0$ for $b > a$.

The deflection angle often resembles the behavior shown in Figure A1.2 as a function of impact parameter. For large impact parameters, χ is small and negative (net attraction), and as b decreases, the deflection becomes more negative (increasing attraction). The deflection then either approaches negative infinity, corresponding to *classical orbiting*, or reaches a finite minimum. Classical orbiting occurs when the impact parameter equals the maximum in the centrifugal barrier and the initial velocity is such that the (radial) velocity vanishes at the maximum in the centrifugal barrier. For still smaller impact parameters, the effect of the short-range repulsive part of the potential causes the deflection angle to increase, passing through zero (where net attraction and repulsion cancel) and finally to approach 180° as $b \to 0$. As Eq. (17) shows, the differential cross section becomes singular when either $\chi = 0°$, called *forward glory scattering*, or $d\chi/db = 0$ at the minimum, called *rainbow scattering*. The rainbow deflection angle χ_r will depend, of course, on the velocity *v*.

The calculation of the differential cross section is considerably simplified if we consider only those collisions at large impact parameters since they contribute only to scattering at small deflection angles, that is, in the forward direction. Let the initial momentum of the particles be along the *x* axis. Denote by $\mathbf{p}'$ the momentum of the particle after scattering. Then, $p' \sin\chi = p_y'$, and for small deflection angles, we take $\sin\chi \simeq \chi$ and write

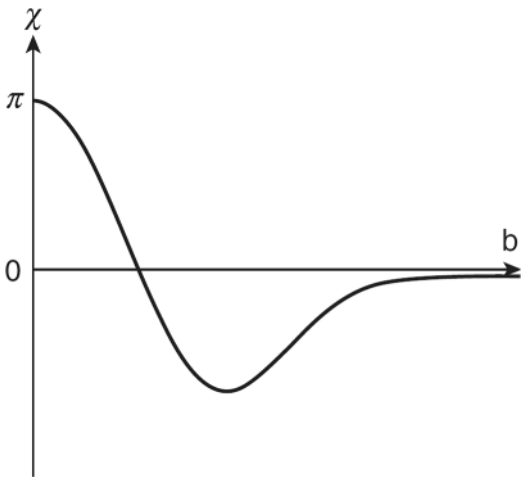

FIGURE A1.2 Deflection angle as a function of the impact parameter (generic form).

$$\chi \simeq \frac{p_y'}{p'} = \frac{\text{momentum transfer}}{\text{momentum}} \tag{19}$$

As the time derivative of the momentum is the force, the momentum transferred perpendicular to the initial direction is given by integrating the force component F_y' over the trajectory. But

$$F_y' = -\left(\frac{\partial V}{\partial y}\right) = -\left(\frac{\partial V}{\partial r}\right)\left(\frac{\partial r}{\partial y}\right) = -\left(\frac{\partial V}{\partial r}\right)\frac{b}{r} \tag{20}$$

where we use the facts that $r^2 = x^2 + y^2$ and $y \simeq b$. Hence

$$\begin{aligned}\chi &= \frac{p_y'}{\mu(2E/\mu)^{1/2}} \\ &= -b(2\mu E)^{-1/2}\int_{-\infty}^{\infty}\left(\frac{\partial V}{\partial r}\right)\frac{dt}{r} \\ &= -b\,(2\mu E)^{-1/2}\left(\frac{2E}{\mu}\right)^{-1/2}\int_{-\infty}^{\infty}\left(\frac{\partial V}{\partial r}\right)\frac{dx}{r} \\ &= -\frac{b}{E}\int_{b}^{\infty}\left(\frac{\partial V}{\partial r}\right)\frac{1}{\sqrt{r^2 - b^2}}dr\end{aligned} \tag{21}$$

where $x = \sqrt{\frac{2E}{\mu}}\,t$ and x varies from $-\infty$ to ∞ as r varies from ∞ to b and back.

D. Use Eq. (21) to examine the small-angle elastic scattering from the potential $V(r) = C_s r^{-s}$ for $s > 0$. Show that

$$\chi = \frac{sC_s\sqrt{\pi}}{2b^s E}\frac{\Gamma[(s+1)/2]}{\Gamma[s/2+1]} \tag{22}$$

from which it is concluded that χE is a function of b alone.

Complete this study by evaluating $I(\chi)$, using Eq. (17) to prove that

$$I(\chi) = \frac{1}{s}\left\{\frac{sC_s\sqrt{\pi}}{2E}\frac{\Gamma[(s+1)/2]}{\Gamma[s/2+1]}\right\}^{2/s}\chi^{-(2+2/s)} \tag{23}$$

for small values of χ. Hence, a log–log plot of the center-of-mass differential scattering cross section $I(\chi)$ as a function of the scattering angle χ at fixed energy should give a straight line with slope $-(2 + 2/s)$ from which the value of the s can be determined [2–5]. For the usual case of neutral closed-shell systems, $s = 6$ (van der Waals long-range attractive potential) and $I(\chi)$ is proportional to $E^{-1/3}\chi^{-7/3}$.

Quantum Treatment

The quantum formulation of scattering in a central force field may be found in many texts [5–11] and is not developed in detail here. Briefly, the scattering is determined by the asymptotic form of the wave function

$$\psi(r,\ \chi) \xrightarrow[r\to\infty]{} A\left[e^{ikz} + \frac{f(\chi)}{r}\, e^{ikr}\right] \tag{24}$$

where A is a normalization constant and

$$k = \frac{1}{\lambda\!\!\!^{-}} = \frac{\mu v}{\hbar} \tag{25}$$

is the magnitude of the initial propagation vector **k** that is directed along $\chi = 0$. In Eq. (24), the term $A\exp(ikz)$ represents a plane wave incident on the scattering center and the term $Af(\chi)\exp(ikr)/r$ represents an outgoing spherical wave. Note that the amplitude of the scattered wave is inversely proportional to r since the radial flux must decrease as the inverse square of the distance. If the incoming and scattered fluxes of particles are separated from each other, by collimating slits, for example, the differential cross section is related to the scattering amplitude $f(\chi)$ by

$$I(\chi) \ = \ |f(\chi)|^2 \tag{26}$$

Thus, the asymptotic form of the wave function determines the differential scattering cross section but cannot be found without solving the wave equation throughout all space. This may be carried out by the method of partial waves in which the general solution is represented as an infinite sum of Legendre polynomials

$$\psi(r,\ \chi) = \sum_{\ell=0}^{\infty} R_\ell(r) P_\ell(\cos\chi) \tag{27}$$

The boundary condition that $R_\ell(r)$ remains finite at $r = 0$ determines the asymptotic form of the solution, up to the normalization constant.

In the absence of a potential $V(r) = 0$, the wave function is simply $A\exp(ikz)$, which can be cast into the form of Eq. (27) for large r as

$$e^{ikz} \xrightarrow[r\to\infty]{} \sum_{\ell=0}^{\infty} (2\ell+1)\ \exp\left(\frac{i\ell\pi}{2}\right) \frac{\sin\left(kr - \frac{\ell\pi}{2}\right)}{kr} P_\ell(\cos\chi)$$

$$= \frac{1}{2i}\sum_{\ell=0}^{\infty} i^\ell (2\ell+1) P_\ell(\cos\chi) \left\{ \frac{e^{i\left(kr-\frac{\ell\pi}{2}\right)}}{kr} - \frac{e^{-i\left(kr-\frac{\ell\pi}{2}\right)}}{kr} \right\} \tag{28}$$

Equation (28) has an appealing physical interpretation, namely, the incident plane wave is equivalent to a superposition of an infinite number of incoming and outgoing spherical waves in which each term in Eq. (28) corresponds to an orbital angular momentum of magnitude

$$L = \sqrt{\ell(\ell+1)}\hbar \simeq \left(\ell + \frac{1}{2}\right)\hbar \tag{29}$$

about the scattering center. Classically, this angular momentum would correspond to an impact parameter

$$b = \frac{L}{\mu v} \simeq \frac{\left(\ell+\frac{1}{2}\right)}{k} = \left(\ell + \frac{1}{2}\right)\lambda\!\!\!^{-} \tag{30}$$

Thus, we can picture the incident beam as divided into cylindrical zones such that the ℓth zone contains particles with impact parameters between $\ell\lambda\!\!\!^{-}$ and $(\ell+1)\lambda\!\!\!^{-}$.

E. In quantum mechanics only integral values of ℓ are allowed, yet we view b as being continuous. How will this affect our results when treating chemical systems?

Provided $V(r)$ falls off more rapidly than $1/r$ for large r, the general solution [Eq. (27)] can be shown to have the asymptotic form

$$\psi(r,\ \chi) \xrightarrow[r\to\infty]{} \sum_{\ell=0}^{\infty}(2\ell+1)\ \exp\left[i\left(\frac{\ell\pi}{2}+\eta_\ell\right)\right]\frac{\sin\left(kr-\frac{\ell\pi}{2}+\eta_\ell\right)}{kr}P_\ell(\cos\chi)$$

$$= \frac{1}{2i}\sum_{\ell=0}^{\infty} i^\ell(2\ell+1)P_\ell(\cos\chi)\left\{e^{2i\eta_\ell}\frac{e^{i\left(kr-\frac{\ell\pi}{2}\right)}}{kr} - \frac{e^{-i\left(kr-\frac{\ell\pi}{2}\right)}}{kr}\right\} \tag{31}$$

where η_ℓ is called the *phase shift* and must be a real number. Comparing Eq. (31) with the solution for $V(r) = 0$, namely, Eq. (28), we conclude that the effect of the scattering potential is to introduce a change of phase in the asymptotic form of the radial wave functions. Moreover, the phase shift occurs only in the outgoing part of the asymptotic wave function. This is indicated schematically in Figure A1.3. A repulsive potential causes a decrease in the relative velocity of the particles for small r so that the wavelength is increased. Thus, the scattered wave is "pushed out" relative to that for $V = 0$, and consequently the phase shift η_ℓ is negative. An attractive potential "pulls in" the radial wave function and produces a positive phase shift. Comparing $\ell = 0$ to $\ell \neq 0$, we also see that the repulsive centrifugal potential contributes a negative phase shift of $-\ell\pi/2$.

Further analysis shows that the scattering amplitude is given by

$$f(\chi) = \frac{1}{2ik}\sum_{\ell=0}^{\infty}(2\ell+1)\left(e^{2i\eta_\ell}-1\right)P_\ell(\cos\chi) \tag{32}$$

which may be derived by comparing Eqs. (24), (28), and (31). Then, the differential cross section has the form

$$I(\chi) = \lambda\!\!\!^{-2}\left|\sum_{\ell=0}^{\infty}(2\ell+1)e^{i\eta_\ell}\sin\eta_\ell\,P_\ell(\cos\chi)\right|^2 \tag{33}$$

Equation (33) shows that interference between the terms with different values of ℓ plays an important role in determining the differential cross section. In terms of our previous picture, the outgoing partial waves scattered from the various zones of incident impact parameters are superimposed with weighting factors that depend on the phase shift associated with each zone. Whenever the phase shift is zero or an integral multiple of π, the corresponding partial wave does not contribute to the scattering, since it has been "pushed out" or "pulled in" an integral number of half wavelengths so that the nodes and extrema in its asymptotic form match those of the incident partial wave, that is, the $V(r) = 0$ solution.

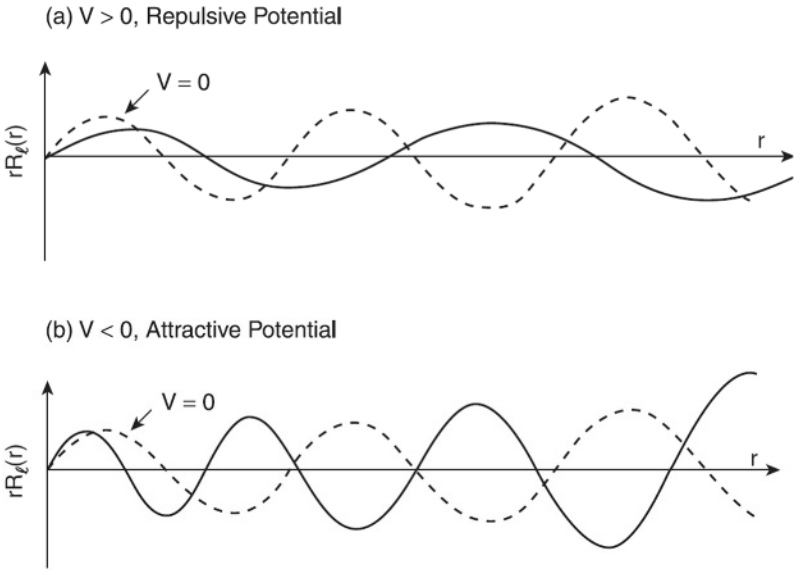

FIGURE A1.3 Form of the radial wave function (solid curve) versus separation distance for (a) a repulsive potential $(V(r) > 0)$ *and (b) an attractive potential* $(V(r) < 0)$. *For comparison, the radial wave function (dashed curve) for no potential* $(V(r) = 0)$ *is also shown.*

The total cross section is obtained by integrating Eq. (33) over all directions:

$$\sigma = 2\pi \int_0^{\pi} I(\chi) \sin\chi \, d\chi = 4\pi \lambda\!\!\!^{-2} \sum_{\ell=0}^{\infty} (2\ell + 1) \sin^2 \eta_\ell \tag{34}$$

Cross terms in the expansion of Eq. (33), which represent the interference of different partial waves, cancel on integration because of the orthogonality of the Legendre polynomials. Equation (34) shows that each partial wave contributes separately to σ in proportion to $\sin^2 \eta_\ell$ and its statistical weight $(2\ell + 1)$. The coefficient 4π represents the integral over the solid angle of scattering, while $\lambda\!\!\!^{-2} = (\lambda/2\pi)^2 = 1/k^2$ is associated with the squared wavelength of the incident particles. From another viewpoint, however, the physical interpretation of Eq. (34) is somewhat strange. The flux of particles incident with impact parameters within the ℓth zone is proportional to the cross-sectional area of the zone, namely, $\pi\lambda\!\!\!^{-2}\left[(\ell + 1)^2 - \ell^2\right] = \pi\lambda\!\!\!^{-2}(2\ell + 1)$. This disagrees with Eq. (33) by a factor of 4. Actually, this factor is the result of quantum mechanical diffraction effects that are not properly included in our simple physical picture. Nevertheless, we did find the correct form in which a $\sin^2 \eta_\ell$ weighting factor appears to express the effectiveness of the potential in scattering the ℓth partial wave.

The uncertainty principle provides a clarification concerning the convergence of Eq. (18) for the total cross section. In a classical treatment, σ diverges unless the potential vanishes outside some finite radius. If the potential extends to infinity, then even very large values of the impact parameter b produce a small deflection and thus contribute to the scattering cross section. However, if the potential is sufficiently weak at large r, the collisions with large impact parameters produce such slight deflections that the scattering angle χ is smaller than the directional uncertainty required by the uncertainty principle. For such collisions, the particle cannot be regarded as scattered, and thus the uncertainty principle, in effect, causes a cutoff in the impact parameter b that can contribute to the scattering process, making the total cross section finite. This is yet another example where quantum mechanics rounds off a classical singularity.

Let us make these considerations more quantitative. There is a largest value of b, denoted by b_c, for which χ is just large enough to be observable. Let $\Delta p'_y$ be the uncertainty in the transverse component of the momentum. Then, according to the uncertainty principle, $b_c \Delta p'_y = h$ or $\Delta p'_y = \frac{h}{b_c}$. Thus, it follows from Eq. (19) that the deflection angle χ_c associated with b_c must be

$$\chi_c = \frac{\Delta p'_y}{p} = \frac{h}{b_c \sqrt{2\mu E}} \tag{35}$$

However, we also found according to Eq. (22) that for a potential of the form $V(r) = C_s r^{-s}$, χ_c is related to the impact parameter b_c by

$$\chi_c = \frac{s\, C_s \sqrt{\pi}\, \Gamma[(s+1)/2]}{2\, b_c^s\, E\, \Gamma[s/2+1]} \tag{36}$$

combining Eqs. (35) and (36), we have

$$b_c = \left[\frac{s\, C_s \sqrt{\pi} \Gamma[(s+1)/2]}{h\, \upsilon\, \Gamma[s/2+1]}\right]^{\frac{1}{(s-1)}} \tag{37}$$

where υ is the initial velocity. It follows that the cross section cannot exceed πb_c^2 and its velocity dependence is $\upsilon^{-2/(s-1)}$. For $s = 6$, $\sigma(\upsilon)$ is proportional to $\upsilon^{-2/5}$.

Actually, an undulatory velocity dependence of $\sigma(\upsilon)$ is often observed superimposed on the general trend predicted above [2–5]. This is brought about by the quantum interference arising from trajectories at very large impact parameters ($b \geq b_c$) and glory trajectories $b \simeq b_g$ as both contribute to $\chi \leq \chi_c$. Nevertheless, a plot of $\ln \sigma(\upsilon)$ versus $\ln \upsilon$ can be used to reveal the power law behavior of the long- and short-range parts of the potential and even to obtain an estimate of C_s.

To illustrate this procedure, we present in Figure A1.4 the velocity dependence of the total cross section when a velocity-selected beam of K crosses a thermal beam of Cs, Hg, Xe, Kr, or Ar [see D. Beck and H. J. Loesch, *Z. Phys*., **195**, 444 (1966)]. The data, which have been corrected for the velocity distribution of the target gas, show a slope close to $-2/5$, the value expected for an $s = 6$ long-range attractive potential. Glory scattering undulations in the total cross section are also apparent. The amplitudes of the glory undulations contain information on the width of the potential well. Total and differential cross section

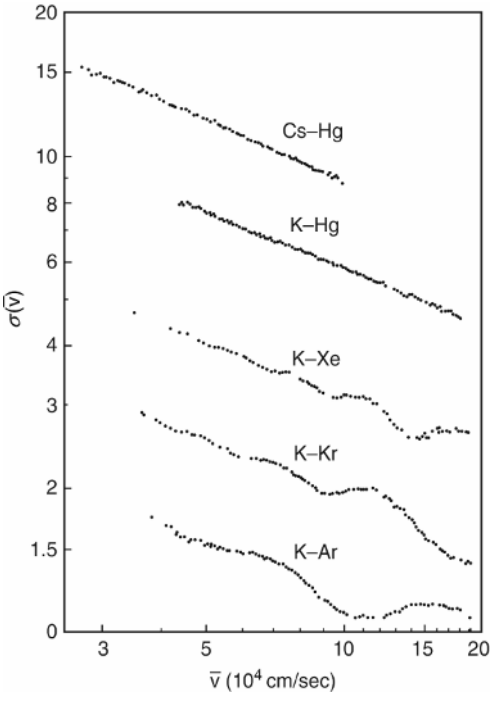

*FIGURE A1.4 Reprinted with permission from D. Beck and H. J. Loesch, Z. Phys., **195**, 444 (1966).*

measurements have been widely used to obtain information about intramolecular potential energy functions [2–5].

Transition from Quantum to Classical Scattering

The phase shift, which so naturally arises in a quantum description of the scattering process, may also be defined semiclassically by comparing the number of wavelengths contained in two different paths, the actual trajectory, and the path that would be followed if the scattering potential were "switched off":

$$\eta_\ell^{\mathrm{SC}} = \lim_{R\to\infty}\left[\int_{r_c}^{R}\frac{dr}{\lambda\!\!\!^{-}_r} - \int_{b}^{R}\frac{dr}{\lambda\!\!\!^{-}_r}\right] \tag{38}$$

Here, R is the radius of a sphere whose center coincides with the scattering center, and

$$\lambda\!\!\!^{-}_r = \frac{\hbar}{\mu\dot{r}} = \frac{\hbar}{\mu v\sqrt{1 - V(r)/E - b^2/r^2}} \tag{39}$$

is the "local" de Broglie wavelength associated with the radial motion. Thus, the semiclassical phase shift is given by

$$\eta_\ell^{\mathrm{SC}} = k\left\{\int_{r_c}^{\infty}\left[1 - \frac{V(r)}{E} - \frac{b^2}{r^2}\right]^{\frac{1}{2}} dr - \int_{b}^{\infty}\left[1 - \frac{b^2}{r^2}\right]^{\frac{1}{2}} dr\right\} \tag{40}$$

This formula can be put in a more familiar form by introducing $k_r = \mu\dot{r}/\hbar$ and rewriting Eq. (38) as

$$\eta_\ell^{\mathrm{SC}} = \lim_{R\to\infty}\left[\int_{r_c}^{R} k_r dr - \int_{r_c}^{R} k dr + \int_{r_c}^{R} k dr - \int_{b}^{R} k\left(1 - \frac{b^2}{r^2}\right)^{\frac{1}{2}} dr\right] \tag{41}$$

The last integral is readily evaluated:

$$k\int_{b}^{R}\frac{\sqrt{r^2 - b^2}\,dr}{r} = k\left[\sqrt{r^2 - b^2} - b\arccos\frac{b}{r}\right]\Bigg|_{b}^{R} = kR - \frac{kb\pi}{2} \tag{42}$$

Hence,

$$\eta_\ell^{\mathrm{SC}} = \lim_{R\to\infty}\left[\int_{r_c}^{R}(k_r - k)dr + k(R - r_c) - k(R - b\pi/2)\right]$$
$$= \int_{r_c}^{\infty}(k_r - k)dr - k(r_c - b\pi/2)$$
$$= \int_{r_c}^{\infty}(k_r - k)dr - k\,r_c + \left(\ell + \tfrac{1}{2}\right)\tfrac{\pi}{2} \qquad (43)$$

which is the standard form for the semiclassical phase shift as given in many quantum mechanics texts [5–11].

The deflection angle χ may also be expressed in a form resembling that for η_ℓ^{SC} by writing

$$\chi = \lim_{\mathrm{R}\to\infty}\left[\left(\pi - 2\int_{\substack{\text{actual}\\ \text{path}}} d\theta\right) - \left(\pi - 2\int_{\substack{\mathrm{V}=0\\ \text{path}}} d\theta\right)\right]$$
$$= -2b\left[\int_{r_c}^{\infty}\left[1 - \frac{V(r)}{E} - \frac{b^2}{r^2}\right]^{-1/2}\frac{dr}{r^2} - \int_{b}^{\infty}\left(1 - \frac{b^2}{r^2}\right)^{-1/2}\frac{dr}{r^2}\right] \qquad (44)$$

Equation (44) may seem a peculiar way to express χ, and it might be wondered why bother. After all, the last integral in Eq. (44) is

$$\int_{b}^{\infty}\frac{dr}{r\sqrt{r^2 - b^2}} = \left[\frac{1}{b}\arccos\frac{b}{r}\right]\Bigg|_{b}^{\infty} = \frac{1}{b}\left(\frac{\pi}{2}\right) \qquad (45)$$

so that Eq. (44) reduces to Eq. (14). However, Eq. (44) allows us to deduce a simple and useful connection between the classical deflection angle χ and the rate of change of the semiclassical phase shift with angular momentum, $d\eta_\ell^{\mathrm{SC}}/d\ell$. Recall that the general rule for differentiating a definite integral is

$$\frac{d}{dx}\int_{a(x)}^{b(x)} f(x,y)dy = \frac{db(x)}{dx}f[x,b(x)] - \frac{da(x)}{dx}f[x,a(x)] + \int_{a(x)}^{b(x)}\frac{\partial f(x,y)}{\partial x}\,dy \qquad (46)$$

By differentiating Eq. (40) with respect to ℓ and using Eq. (46) and the relation $\left(\frac{\partial b}{\partial \ell}\right)_E = \frac{1}{k}$, we find that

$$\frac{d\eta_\ell^{\mathrm{SC}}}{d\ell} = \frac{1}{2}\chi \qquad (47)$$

Next let us examine the differential cross section $I(\chi)$. The mathematical identity

$$\delta(1-\cos\chi)=\frac{1}{2}\sum_{\ell=0}^{\infty}(2\ell+1)P_\ell(\cos\chi) \tag{48}$$

is readily verified. If we exclude the singular point $\chi = 0$, which contributes negligibly to the total flux, we can rewrite Eq. (32) as

$$f(\chi)=\frac{\lambda\!\!\!^{-}}{2i}\sum_{\ell=0}^{\infty}(2\ell+1)\ \exp(2i\eta_\ell)\,P_\ell(\cos\chi) \tag{49}$$

To obtain the classical limit, we consider the situation where the potential varies slowly over distances comparable to the de Broglie wavelength and that many ℓ values contribute to the scattering at a given angle so that the major contribution arises from large ℓ values. Then, for $\chi \neq 0$,

$$f(\chi)=-\lambda\!\!\!^{-}\sum_{\ell=0}^{\infty}\left[\frac{\left(\ell+\frac{1}{2}\right)}{2\pi\sin\chi}\right]^{\frac{1}{2}}\left[\exp(i\phi^{+})-\exp(i\phi^{-})\right] \tag{50}$$

where

$$\phi^{\pm}=2\eta_\ell\pm\left(\ell+\tfrac{1}{2}\right)\chi\pm\tfrac{1}{4}\pi \tag{51}$$

F. Derive Eq. (50).

Hint: Reread Note [8] of Chapter 1.

In Eq. (50) the exponential factors are rapidly oscillating functions of ℓ, as the phases $\phi^{\pm}$ are large. Thus, the majority of terms cancels, and this sum is determined mainly from the range of ℓ values for which either ϕ^{+} or ϕ^{-} is an extremum. From Eq. (51) this implies that Eq. (50) is essentially determined only by phase shifts satisfying the relation

$$\frac{2d\eta_\ell}{d\ell}\pm\chi=0 \tag{52}$$

where the plus sign is for $d\phi^{+}/d\ell = 0$ and the minus sign for $d\phi^{-}/d\ell = 0$. Comparison of Eq. (52) with Eq. (47) demonstrates that only these phase shifts η_ℓ corresponding to the impact parameter b contribute to the differential cross section $I(\chi)$ in the classical limit. Conversely, the condition for classical scattering at a given deflection angle χ is that the values of ℓ be large for which Eq. (52) applies.

We conclude by examining one of the most striking phenomena in scattering, namely, *resonance scattering*, in which the total cross section shows an abrupt change as a function of energy. As shown in Eq. (34), each partial wave ℓ contributes to the total cross section a term

$$\sigma_\ell = \frac{4\pi}{k^2}(2\ell + 1)\ \sin^2\eta_\ell \tag{53}$$

Generally, the phase shifts η_ℓ are slowly varying functions of the energy. A resonance occurs for some partial wave ℓ when η_ℓ changes rapidly over a small energy range, and we write

$$\eta_\ell(E) = \eta_{\text{bg}} + \eta_{\text{res}} \tag{54}$$

where η_{bg} is the background phase shift, and η_{res} is the resonance phase shift.

What makes a resonance occur? To understand this, we turn our attention to Eq. (31), the asymptotic form of the wave function. For a given ℓ, the ratio $S_\ell(k)$ of the outgoing wave amplitude to the incoming wave amplitude at energy $E = \frac{\hbar^2 k^2}{2\mu}$ is

$$S_\ell(k) = e^{2i\eta_\ell(k)} \tag{55}$$

up to a constant factor. Here, we have emphasized the dependence of the phase shift on energy by writing $\eta_\ell = \eta_\ell(k)$. The wave number k is a real variable. However, by the process of analytic continuation, $\eta_\ell(k)$ can be regarded as a function of a complex variable k. Suppose there exists an imaginary value of k, that is

$$k = i\kappa \tag{56}$$

where κ is real and positive definite such that

$$S_\ell(\kappa) = e^{2i\eta_\ell(\kappa)} = 0 \tag{57}$$

Of course, this implies that the energy is negative, and

$$\eta_\ell(\kappa) = i\,\infty \tag{58}$$

that is, the asymptotic behavior of the wave function will go as $\exp\left(-\kappa r + \frac{\ell\pi}{2}\right)/\kappa r$, and there is no outgoing wave amplitude, only an exponentially dying form. This is exactly the condition of a bound state. Thus, the zeros of S_ℓ correspond to bound states. Conversely, when $k = -i\kappa,\ S_\ell$ will grow without bound, and it follows that the poles (singularities in the complex plane) of S_ℓ correspond to scattering resonances. Close to a resonance

$$S_\ell(k) = e^{2i\eta_\ell} = e^{2i\eta_{\rm bg}} \frac{e^{i\eta_{\rm res}}}{e^{-i\eta_{\rm res}}} = e^{2i\eta_{\rm bg}} \frac{1 + i\tan\eta_{\rm res}}{1 - i\tan\eta_{\rm res}} \tag{59}$$

The simplest way of causing S_ℓ to grow without bound near E_0 is to make it have a simple pole, that is, to set

$$\eta_{\rm res} = \arctan\left[\frac{\Gamma/2}{E_0 - E}\right] \tag{60}$$

where the meaning of $\Gamma/2$ will become apparent but for the present may be assumed to be a constant independent of energy. Then, Eq. (59) becomes

$$S_\ell(k) = \frac{(E_0 - E) + i(\Gamma/2)}{(E_0 - E) - i(\Gamma/2)} e^{2i\eta_{\rm bg}} \tag{61}$$

and $S_\ell(k)$ has a pole at $E = E_0 - i(\Gamma/2)$.

When $\eta_{\rm bg}$ can be neglected, substitution of Eq. (60) into Eq. (53) yields the result

$$\sigma_\ell = \frac{4\pi}{k^2}(2\ell + 1)\frac{(\Gamma/2)^2}{(E_0 - E)^2 + (\Gamma/2)^2} \tag{62}$$

where we have made use of the identity

$$\arctan x = \arcsin\frac{x}{\sqrt{x^2+1}} \tag{63}$$

Equation (62) is called the *Breit–Wigner formula* [12] for an isolated scattering resonance. It describes a bell-shaped curve with a half-width at half-maximum of $\Gamma/2$. This suggests that the occurrence of a resonance at E_0 in the partial cross section σ_ℓ is associated with the formation of a virtual state (metastable bound state) with energy E_0 and width Γ. Moreover, in analogy to a bound state, the time dependence of this virtual state (scattering resonance) is given by $\exp[-i(E_0 - i\Gamma/2)t/\hbar]$ so that it is characterized by a lifetime $\tau = \hbar/\Gamma$.

In the more general case, $\eta_{\rm bg}$ cannot be ignored and there is interference between the background and resonance phase shifts. Figure A1.5 shows plots of $\sin^2\eta_\ell(E)$ as a function of E for $\eta_{\rm bg} = 0.0$ and $\eta_{\rm bg} = \frac{\pi}{10}$, assuming that Γ is independent of E over the resonance.

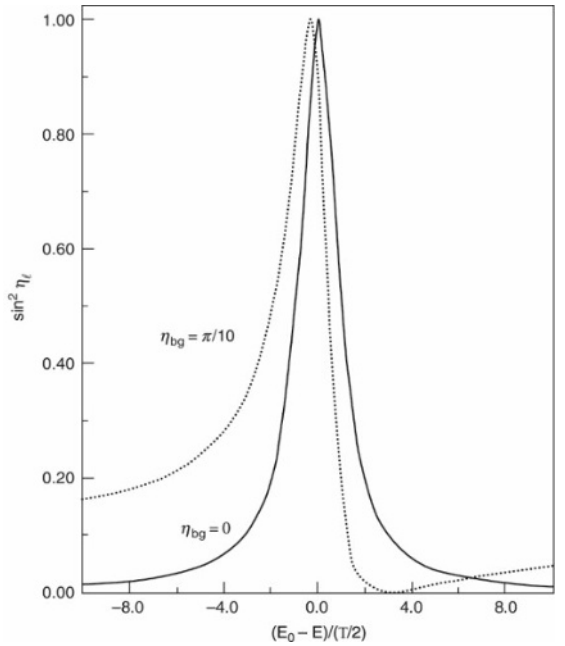

FIGURE A1.5 Line profile of an isolated scattering resonance for two different background phase shifts, $\eta_{bg} = 0$ and $\eta_{bg} = \frac{\pi}{10}$. Note that when $\eta_{bg} \neq 0$ it is possible for the cross section to vanish at a particular energy (the so-called Cooper minimum).

G. Show that the partial cross section is then given by

$$\sigma_\ell = \frac{4\pi}{k^2}(2\ell+1)\sin^2\left[\eta_{\mathrm{bg}} + \arctan\left(\frac{\Gamma/2}{E_0 - E}\right)\right]$$
$$= \frac{4\pi}{k^2}(2\ell+1)\frac{(\varepsilon+q)^2}{1+\varepsilon^2}\sin^2\eta_{\mathrm{bg}} \tag{64}$$

where

$$\varepsilon = \frac{E_0 - E}{\Gamma/2} \tag{65}$$

is the energy difference measured in half-widths and

$$q = \cot\eta_{\mathrm{bg}} \tag{66}$$

is called the line profile index.

It has been shown by Fano [13] and Fano and Cooper [14] that absorption lines in photoionization may have profiles as illustrated above. Again, this arises from interference between the continuum states produced by nonresonant photon absorption and the continuum state produced by the decay of a resonance.

One of the commonest situations that cause the appearance of resonances is an effective potential that is composed of an attractive part at small distances and a repulsive centrifugal barrier at long distances, as shown in Figure A1.6. For energies below the

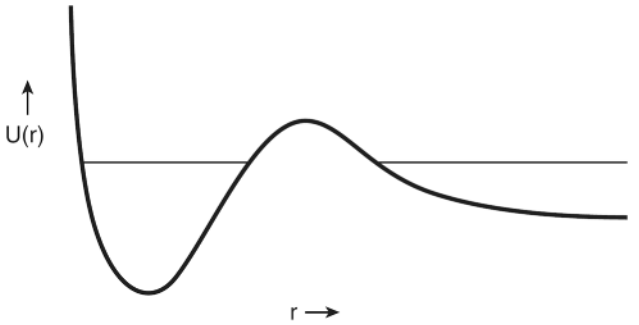

FIGURE A1.6 Plot of the potential energy including the centrifugal potential versus separation distance.

maximum in the centrifugal barrier, there would be bound states inside the attractive part of the potential if tunneling could be ignored.

However, the presence of quantum mechanical tunneling permits particles "trapped" inside the attractive part of the potential to escape to infinity, and the tunneling rate depends on the height and thickness of the barrier. Conversely, particles incident on the potential at energy close to the virtual state energy can penetrate inside the attractive barrier. This behavior explains why resonances generally become narrower as ℓ increases. Larger ℓ values cause bigger centrifugal barriers, thus suppressing tunneling.

NOTES AND REFERENCES

1. J. O. Hirschfelder, R. F. Curtiss, and R. B. Bird, *Molecular Theory of Gases and Liquids*, Wiley, New York, 1954.

2. G. C. Maitland, M. Rigby, E. B. Smith, and W. A. Wakeham, *Intramolecular Forces*, Clarendon Press, Oxford, 1981.

3. R. B. Bernstein, *Chemical Dynamics via Molecular Beam and Laser Techniques*, Clarendon Press, Oxford, 1982, Chapter 5; *Adv. Chem. Phys*., **10**, 75 (1966).

4. J. P. Toennies, "Molecular Beam Scattering Experiments on Elastic, Inelastic, and Reactive Collision," in *Physical Chemistry*, Vol. VIA, H. Eyring, D. Henderson, W. Jost, eds., Academic Press, New York, 1974, Chapter 5.

5. M. S. Child, *Molecular Collision Theory*, Academic Press, New York, 1974.

6. H. S. W. Mott and N. F. Massey, *The Theory of Atomic Collisions*, 3rd ed., Clarendon Press, Oxford, 1965.

7. R. G. Newton, *Scattering Theory of Waves and Particles*, McGraw-Hill, New York, 1966.

8. L. I. Schiff, *Quantum Mechanics*, 3rd ed., McGraw-Hill, New York, 1968.

9. L. D. Landau and E. M. Lifshitz, *Quantum Mechanics*, Addison-Wesley, Reading, MA, 1958.

10. J. R. Taylor, *Scattering Theory*, Wiley, New York, 1972.

11. U. Fano and A. R. P. Rau, *Atomic Collisions and Spectra*, Academic Press, Orlando, 1986.

12. G. Breit and E. Wigner, *Phys. Rev*., **49**, 519 (1936).

13. U. Fano, *Phys. Rev*., **124**, 1866 (1961).

14. U. Fano and J. W. Cooper, *Phys. Rev.*, **137**, A1364 (1965); *Rev. Mod. Phys.*, **40**, 441 (1968).